

Progress of 2D MXene as an Electrode Architecture for Advanced Supercapacitors: A Comprehensive Review

Anu Mini Aravind, Merin Tomy, Anupama Kuttapan, Ann Mary Kakkassery Aippunny, and Xavier Thankappan Suryabai*

Cite This: *ACS Omega* 2023, 8, 44375–44394

Read Online

ACCESS |

Metrics & More

Article Recommendations

ABSTRACT: Supercapacitors, designed to store more energy and be proficient in accumulating more energy than conventional batteries with numerous charge–discharge cycles, have been developed in response to the growing demand for energy. Transition metal carbides/nitrides called MXenes have been the focus of researchers' cutting-edge research in energy storage. The 2D-layered MXenes are a hopeful contender for the electrode material due to their unique properties, such as high conductivity, hydrophilicity, tunable surface functional groups, better mechanical properties, and outstanding electrochemical performance. This newly developed pseudocapacitive substance benefits electrochemical energy storage because it is rich in interlayer ion diffusion pathways and ion storage sites. Making MXene involves etching the MAX phase precursor with suitable etchants, but different etching methods have distinct effects on the morphology and electrochemical properties. It is an overview of the recent progress of MXene and its structure, synthesis, and unique properties. There is a strong emphasis on the effects of shape, size, electrode design, electrolyte behavior, and other variables on the charge storage mechanism and electrochemical performance of MXene-based supercapacitors. The electrochemical application of MXene and the remarkable research achievements in MXene-based composites are an intense focus. Finally, in light of further research and potential applications, the challenges and future perspectives that MXenes face and the prospects that MXenes present have been highlighted.



1. INTRODUCTION

The declining use of fossil fuels and the increasing use of energy have sparked interest in renewable energy sources. Due to climatic changes, relying solely on these energy sources is impossible. Consequently, there is an urgent need for renewable and endless energy sources.¹ It leads to multifunctional electrochemical energy storage devices with safety, high stability, and high power density.² The widespread acceptance of rechargeable batteries results from their extended lifespan and increased energy density.^{3,4}

Nevertheless, an ideal power source that stores energy and produces a sound output is practically unfeasible. In this scenario, developing energy storage systems using diverse technologies is essential. Supercapacitors (SCs) or electrochemical capacitors have emerged as a class of new-generation storage systems that can fulfill the growing demands in the high-energy field because of their high-power density and long-term stability.^{5,6} Supercapacitors are divided into electrical double-layer capacitors (EDLCs), pseudocapacitors, and hybrid capacitors based on how energy storage and ions move from the electrode to the electrolyte.^{7,8} Carbonaceous materials are frequently used for EDLCs, including carbon nanotubes (CNTs), graphene, and activated carbon.^{9,10} Metal oxides, nitrides, sulfides, conducting polymers, and tellurides are

suitable electrode materials for pseudocapacitors.^{10,11} Figure 1 shows the schematic representation of a supercapacitor.

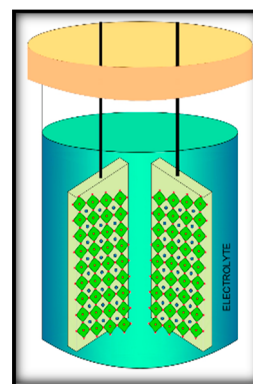


Figure 1. Schematic diagram of a supercapacitor.

Received: April 2, 2023
Revised: October 16, 2023
Accepted: October 26, 2023
Published: November 14, 2023



High-performance electrodes with a large surface area, high electrical conductivity, a long life span, and a uniform pore size distribution are needed.⁹ Therefore, research on new electrode materials with high performance is ongoing and worthwhile. Among several electrodes, 2D inorganic materials are prominent due to their unique physical, chemical, optical, and electrical properties like high morphological anisotropy and a special quantum effect.¹² Simultaneously, some 2D materials, such as covalent–organic frameworks, metal–organic frameworks, metal oxides, and MXenes for supercapacitors, are gaining prominence.¹³ Among them, MXenes were discovered by Gogotsi and Barsoum in 2011 and have been proven as effective pseudocapacitive electrode materials with high capacitance, a large surface area, and long cyclic stability.^{10,14,15} They successfully synthesized Titanium Carbide MXene (TiC_2T_x) by the selective etching of raw Titanium Aluminum Carbide (Ti_3AlC_2). It became the researcher's favorite material due to its tunable properties, like its 2D structure with atomic thickness, electrical conductivity, mechanical strength, and excellent performance in many applications, including sensors, medicine, etc.^{12,16,17}

Despite the synthesis of over 30 MXenes and 70 MAX phases in the scientific field, the initial MXenes captured the spotlight, leading to the rapid expansion of this family of 2D materials.^{18–20} MXenes are currently facing challenges in attaining the desired level of flexibility for wearable technology. Despite ongoing efforts, certain issues persist in their journey toward achieving the requisite flexibility for wearable technology. The conventional etching method of MXene by hydrochloric acid has some defects and requires improvement.²¹ Due to their propensity for compact packing, MXene sheets hinder the movement and diffusion of electrolyte ions, particularly organic ones. It impacts the ability of MXenes to store energy in supercapacitors and limits their electrochemical performance.²² However, MXenes are readily oxidized at higher anode potentials, decreasing cycle efficiency and longevity.²³ The rational design and manufacturing of composite electrodes based on MXene are considered effective solutions to the above-mentioned issues. Shao et al. conducted work to understand the pseudocapacitive behavior of $\text{Ti}_3\text{C}_2\text{T}_x$ MXene in H_2SO_4 electrolyte.²⁴ Shi et al. proposed a braided coaxial zinc–ion hybrid FSC with several meters of $\text{Ti}_3\text{C}_2\text{T}_x$ MXene cathode as core electrodes, and the shell zinc fiber anode was braided on the surface of the $\text{Ti}_3\text{C}_2\text{T}_x$ MXene fibers across the solid electrolytes and exhibited a high areal capacitance of 214 mF cm^{-2} , an energy density of $42.8 \mu\text{Wh cm}^{-2}$ at 5 mV s^{-1} , and excellent cycling stability with 83.58% capacity retention after 5000 cycles.²⁵

MXene-based $\text{Ti}_3\text{C}_2\text{Cl}_2$ nanodot-interspersed MXene@NiAl-layered double hydroxide hybrid electrodes with superior pseudocapacitor storage performance have been elaborately designed and electrostatically assembled, exhibiting a super specific capacitance of 2010.8 F/g at 1.0 A/g and high energy density of 100.5 Wh/kg at a power density of 299.8 W/kg .²⁶ Feng et al. synthesized N-doped $\text{Ti}_3\text{C}_2\text{T}_x$ electrode material with an energy density of 51.1 Wh/kg at a power density of W/kg .²⁷ MXene–carbon composites can be employed to create highly flexible supercapacitors with effective electrochemical characteristics.²⁸ Liang et al. analyzed the cyclic voltammetry data in Na_2SO_4 electrolyte for $\text{Ti}_3\text{C}_2\text{T}_x$ –MCNT electrodes, showing that areal capacitance of 1.93 F/cm^2 is substantially higher than literature results for pure $\text{Ti}_3\text{C}_2\text{T}_x$ and $\text{Ti}_3\text{C}_2\text{T}_x$ composites.²⁹ $\text{Ti}_3\text{C}_2\text{T}_x$ NSs are used as the assembly unit in a coagulation bath of IPA and distilled water containing 5 wt % CaCl_2 to create

high-performance fiber supercapacitors with low corrosion. This results in a meter-long $\text{Ti}_3\text{C}_2\text{T}_x$ fiber with exceptional electrical conductivity and mechanical flexibility.³⁰ Liu et al. investigated the electrochemical properties of Co_3O_4 -decorated 3D MXene/rGO hybrid aerogels with a maximum capacitance of 345 F/g at 1 A/g for the porous aerogel electrode.³¹ Patra et al. fabricated a two-electrode symmetric device using $\text{Ti}_3\text{C}_2\text{T}_x$ MXene and passivated vertical graphene nanosheets (VGNs) as a current collector and displayed a high areal capacitance of 199 mF/cm^2 at 0.08 mA/cm^2 along with an excellent stability and efficiency of 90% and nearly 100% over 6000 repetitive charge–discharge cycles.³² The MXene–metal oxide composites have high electrical conductivity, greater volumetric capacitance, and electrochemical stability, making them apt electrode materials for flexible supercapacitors.^{33,34} The electrochemical efficiency of MXenes varies with the thickness of the electrode. One approach to overcoming this challenge is by creating composites of MXene with the polymer.^{35,36} Yuan et al. synthesized the MXene/CNF/PANI composite as a suitable electrode for high-performance supercapacitors.³⁷ A novel water-free etching method has free layered $\text{Ti}_3\text{C}_2\text{T}_x$ MXenes in deep eutectic solvents at room temperature and exhibits splendid specific capacitance of 320 F/g at 2 mV/s .³⁸ The $\text{Ti}_3\text{C}_2\text{T}_x/\text{NiCo}_2\text{S}_4$ asymmetric device exhibits a maximum areal/gravimetric capacitance of $48.6 \text{ mF cm}^{-2}/54.57 \text{ F g}^{-1}$ at $2 \text{ mA cm}^{-2}/2 \text{ A g}^{-1}$ of current density within the wider potential window of 1.4 V .³⁹ For those new to the field, a timely update on electrode material research and development, the creation of novel capacitor configurations, and a discussion of theoretical aspects would be helpful.

Due to their intrinsic conductivity, the possibility of charge transfer made possible by the transition metal M's changing oxidation number, and their distinctive stacking structure, MXenes exhibit exceptional electrochemical properties and are desirable for energy storage applications. MXene finds application across various market segments, including supercapacitors, batteries, electromagnetic shielding, catalysts, gas sensors, water purification, etc. Many papers and reviews on MXene and its synthesis, modifications, and applications have been published. The design process for enhancing the MXene layer has advanced to date. We look forward to the ongoing evolution of fundamental concepts and technical innovation linked to MXenes, which is expected to unveil even more captivating discoveries. Herein, we review the recent research on MXenes and their noteworthy achievements in the realm of supercapacitors. We summarize the structure and properties of MXene. It covers different synthesis methods and highlights their significant advantages. The review thoroughly discusses the working principle, applications, and electrochemical properties of differently synthesized MXene. As the core part of this review, influencing factors depending on electrochemical performance are thoroughly discussed. Further, we focus on the most topical developments in MXene-based composites and their capacitance values. The development trends, problems, and possibilities of MXene composites for energy storage are collected and prospected to give direction for designing MXene for energy storage and other related applications.

2. INTRODUCTION TO MXENES

MXenes are two-dimensional inorganic compounds that contain transition metal carbides, nitrides, or carbonitrides and are indicated by the chemical formula $\text{M}_{n+1}\text{X}_n\text{T}_x$ ($n = 1, 2, 3$), where M denotes early transition metals such as Zr, Ti, Sc, V, Mo, and

Nb, and x represents carbon or nitrogen. T means the functional group such as $-O$, $-H$, and $-Cl$.^{40,41} Figure 2 shows a periodic

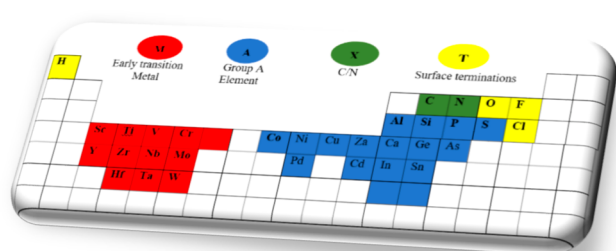


Figure 2. Periodic table illustrating the elements of the MAX phase and MXene.

table illustrating the MAX phase and MXene elements. Due to their negatively charged surface groups, MXenes are hydrophilic and can be dispersed in an aqueous medium without the support of any surfactants.⁴² These surface groups can provide many active sites, which maintain the potential for surface modification and high-efficiency loading of active material.⁴³ It is proven that the energy storage capacity of MXene is powerfully dependent on surface terminal functional groups. F and OH surface terminals decrease energy storage capacity by blocking electrolyte ion transport.⁴⁴ Hu et al. inspected the structural characteristics of oxidized $Ti_3C_2T_x$ and pointed out the importance of surface-terminated groups in electrochemical behavior.⁴⁵ MXenes are synthesized from their parent, known as the MAX phase, a family member of the layered hexagonal with $P63/mmc$ space group.⁴⁶ It has a formula of $M_{n+1}AX_n$ ($n = 1, 2, 3$), where M denotes early transition metals; A denotes group IIIA or IVA elements; and X represents carbon or nitrogen or both.⁴⁷ In most MAX phases, the M–X bond is ionic or covalent, and the M–A bond is metallic. As a result, the M–X bond is more reactive and durable than the M–A bond. Layers were selectively etched from MAX phases using suitable chemicals because of their high reactivity. The M atoms on the surface are terminated with surface groups referred to as T_x . The chemically stable and closely packed MXene ($M_{n+1}X_nT_x$) highlights its properties similar to graphene.^{47,48,42,49,50}

3. SYNTHESIS OF MXENE

3.1. Top-up Method. The top-down approach can be divided into 5 categories⁴¹ based on the etchant. The vital principle to achieve a 2D structure MXene from its respective 3D MAX phase is to fade the interlayer bonds of the 3D structure. The mechanical and chemical etching methods can exfoliate the 3D system for a 2D design.⁴⁹ However, this method is not valid for MXene since the MAX phase's M–A bond is a solid metallic bond that stops the mechanical shearing and hinders the formation of the 2D structure MXene.⁸ Hence, MXene can be synthesized by selective etching or temperature treatment.⁴²

3.1.1. HF Etching. According to reports, Naguib et al. synthesized the first MXene by HF etching.⁵¹ The submerging of MAX phase material accomplishes the exfoliation of A layers from the MAX phase by immersing MAX phase material into an aqueous solution of HF acid, the most widely used etchant.⁸ This process of etching results in the replacement by surface termination groups like $-F$, $-O$, and $-OH$ and multilayered flakes of MXene with 2D layers that van der Waals and hydrogen

bonds organize. Then, sonication facilitates the delamination of distinct MXene layers into multilayered MXene.^{8,52,53} The properties of MXene depend on the HF concentration. A high HF concentration leads to ternary fluoride development, which delays the etching process. Also, it causes structural imperfections and a drop in lateral size.⁵⁴ A low concentration of HF holds more high-mobility water molecules between the interspaces of MXene and gives additional interlayer space and higher capacitance.⁵⁵ Hu et al. synthesized MXene using high and low concentrations of HF and revealed a vast interlayer area and high capacitance for low HF concentrations compared to high HF concentrations.¹⁹ A vacancy-ordered $Mo_{1.3}CT_x$ MXene is formed from $(Mo_{2/3}Sc_{1/3})_2AlC$ by the selective etching of Al and Sc using suitable etchant HF and shows excellent supercapacitor properties.⁵⁶

3.1.2. Fluoride Salt Etching. Some of the etchants include fluoride and difluoride-containing salts like LiF, $NaHF_2$, NH_4F , NH_4HF_2 , CaF_2 , NaF, and KF that are friendly to their surroundings and are used to etch MAX precursors by the intercalation of metal cations and molecules of water and have some advantages over HF.⁵⁷ A mild etchant solution of lithium fluoride (LiF) and hydrochloric acid (HCl) can still be used for the *in situ* production of a less toxic etching solution containing traces of HF in addition to the HF etchant.^{58,59} Figure 3 shows a schematic representation of lithium fluoride etching.



Figure 3. Schematic representation of etching.

In 2014, Ghidui et al. reported the first successfully synthesized Ti_3C_2 by a LiF/HCl solution at 40 °C and obtained a conductive clay with strong plasticity.²² This MXene can be used as an electrode in a supercapacitor with a specific capacity of 900 F cm^{-3} and a minimum capacity loss after 10,000 cycles.^{60,22} An advantage of LiF/HCl etching is that the interlayer spacing of MXene is more extensive than that of HF-etched MXene. It allows faster intercalation of ion movement, resulting in more pseudocapacitive redox sites.^{42,61} Zhang et al. fabricated mesoporous MXene using the LiF etching method, which has an excellent volumetric capacitance of 2079 F/ cm^3 and excellent environmental stability.⁶² Sun et al. synthesized $Ti_3C_2T_x$ MXene by the LiF etchant from the Ti_3AlC_2 MAX phase for an ideal electrode in a supercapacitor.⁶³ Liu et al. synthesized Mo_2CT_x by LiF etching with Mo_2Ga_2C as the MAX phase.⁶⁴

3.1.3. Alkali Etching. The alkali-etching method is acid-free and uses a low alkali concentration to obtain good-quality MXenes. In $M_{n+1}AX_n$, a stronger etchant and longer etching time are needed for higher values of n . Ghidui et al. and colleagues demonstrated that Nb_4AlC_3 ($n = 3$) requires twice the etching time of Nb_2AlC ($n = 3$) under identical etching conditions.⁶⁵ Zhang et al. and Li et al. suggested a NaOH solution as the etchant for an alkali-assisted hydrothermal etching method at a high temperature of 270 °C to synthesize $Ti_3C_2T_x$ MXene.^{66,67} The high concentration of NaOH and high reaction temperature enable the dissolution of aluminum hydroxides in NaOH and

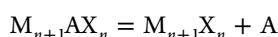
Table 1. Comparison of the Different Synthesis Methods of MXene

MAX phases	Etchants	Etching condition	MXene	Delaminating condition	ref
Ti ₃ AlC ₂	HF	50 wt %, 36 h, 60 °C	Ti ₃ C ₂ T _x	DMSO, 18 h	81
Ti ₃ AlC ₂	HF	50 wt %, 2 h	Ti ₃ C ₂ T _x	centrifugation	82
(Mo _{2/3} Y _{1/3}) ₂ AlC	HF	25 wt %, 120 h	Mo _{1.3} CT _x	TBAOH	56
Nb ₂ AlC	HF	50 wt %, 48 h	Nb ₂ C	Isopropylamine	83
Mo ₂ C	HF	50 wt %, 3 h	Mo ₂ Ga ₂ C		84
V ₂ AlC	HF	48 wt %, 92 h	V ₂ CT _x	TBAOH	85
Ti ₃ AlC ₂	LiF, 9 M HCl	45 °C, 24 h	Ti ₃ C ₂ T _x	sonication	22
Ti ₃ AlC ₂	LiF, 6 M HCl	45 wt %, 45 h	Ti ₃ C ₂ T _x	centrifugation	63
Ti ₃ AlC ₂	LiF, 6 M HCl	40 °C, 45 h	Ti ₃ C ₂ T _x	centrifugation	58
Ti ₃ AlC ₂	1 M NH ₄ HF ₂	Sputtering, 780 °C	Ti ₃ C ₂ T _x		86
Ti ₃ AlC ₂	27.5 M NaOH	Hydrothermal, 270 °C	Ti ₃ C ₂ T _x		66
Ti ₃ AlC ₂	NaOH	Hydrothermal, 100 h	Ti ₃ C ₂ T _x		87
Ti ₃ AlC ₂	KOH	180 °C, 24 h	Ti ₃ C ₂ (OH) ₂		88
Ti ₃ AlC ₂	TMAOH		Ti ₃ C ₂ T _x		89
Ti ₃ AlC ₂	aqueous electrolyte 1 M NH ₄ Cl and 0.2 M TMAOH		Ti ₃ C ₂ T _x		69
Ti ₄ AlN ₃	Molten salts-KF, LiF, NaF	59, 29, 12 wt % 550 °C, 30 min	Ti ₄ N ₃ T _x	sonication	90
Ti ₂ AlC	2 M HCl aqueous electrolyte		Ti ₂ C ₂ T _x		91
Ti ₃ AlC ₂	1 M NH ₄ HF ₂	2.5 V, 2 h	Ti ₃ C ₂ T _x		92
Ti ₃ AlC ₂	1 M NH ₄ Cl 0.1 M TMAOH		Ti ₃ C ₂ T _x		69

hinder the oxidation of Ti. There are qualitative changes in the reaction between the MAX phase and alkali. Because of the low water containment in this reaction system, –O and –OH groups can bind on the surface of Ti₃C₂ MXene except for –F groups.⁶⁸ The fluorine-free MXene can provide more –OH and –O surface terminations that enhance the electrochemical properties of supercapacitors.⁶⁰ Feng et al. conveyed the selective etching of Al layers from Ti₃AlC₂ using an aqueous electrolyte of 1 M ammonium chloride (NH₄Cl) and 0.2 M tetramethylammonium hydroxide (TMAOH), which yields single or bilayer Ti₃C₂T_x MXene that can be used as an electrode.⁶⁹ The etching reaction in an alkaline solution leads to an increase in interlayer spacing and a size reduction, which causes an increase in the active sites of Ti₃C₂T_x MXene and enhancement in cation diffusion. As a result, the e-Ti₃C₂T_x MXene can attain a gravimetric capacitance of 368.1 F/g at a current density of 2 A/⁷⁰

3.1.4. Molten Etching Method. In this process, the reactant and molten salt are arranged into a uniform mixture based on a specific ratio. Heating causes the molten salt to melt, and the reactant completely reacts with the dissolved molten salt.⁷¹ The first 2D transition metal nitride was created by Gogotsi et al. using a fluoride-containing molten salt etching method.⁷² Talapin et al. synthesized and verified Cl/Br-terminated MXene by molten salt etchants cadmium chloride (CaCl₂) and cadmium bromide (CaBr₂), respectively.⁷³

3.1.5. Temperature Etching. The etching process can be more straightforward by the temperature at which metallic bonding of M–A layers can break at high temperatures. The following equation depicts the MAX phase's response under high point temperatures.⁸



Scale-up is difficult due to the acute toxicity of HF, and the management of surface composition and grafting techniques is challenged by competing surface hydrolysis. So, Jawaid et al. present a productive room-temperature etching approach for

producing MXenes from Ti₃AlC₂ using halogens (Br₂, I₂) in anhydrous conditions.⁷⁴ V₂CT_x MXene is synthesized by temperature etching methods at different temperatures, including room temperature.⁷⁵ The synthesis of MXene by temperature etching has been the least explored.

3.1.6. Electrochemical Etching. The electrochemical process for preparing the MXene includes the selective exclusion of A layers from the MAX phase at a particular voltage. The M–A bond's break allows the A layer to be removed in the MAX phase, and MXene is rapidly synthesized at room temperature. It was confirmed that the capacitance of MXene-based supercapacitors after electrochemical etching was greater than that of LiF/HCl-etched MXene.⁷⁶ Yang et al. introduced an efficient fluoride-free etching method based on the anodic decomposition of Al atoms, Ti₃AlC₂, in a binary aqueous electrolyte followed by *in situ* intercalation of ammonium hydroxide. The exfoliated sheets show high volumetric capacitances of 439 F/cm³ at a scan rate of 10 mV/s, more remarkable than LiF/HCl-etched MXene.⁶⁹ Chen et al. devised a facile and time-saving electrochemical method to synthesize –F-free and –Cl-containing Ti₃C₂T_x in a mixed LiOH and LiCl solution with a specific capacitance of 323.7 F/g for supercapacitors.⁷⁷ The comparison of the synthesis techniques is shown in Table 1.

3.2. Bottom-up Method. The bottom-up method can overcome the significant drawbacks of top-down approaches, such as their small size and irregularity. This process can grow MXenes with different heterostructures and free-of-F terminations, which is challenging to compete with the top-down method. MXenes with various heterostructures and free-from-F terminations can be grown by this process, which is hard to achieve with the top-down method. Beyond the top-down approach, bottom-up techniques such as chemical vapor deposition, physical vapor deposition, and the template method are also reported. It is the method to synthesize 2D defect-free monolayer crystals with an excellent area for different applications in electronics and optoelectronics.⁶⁰

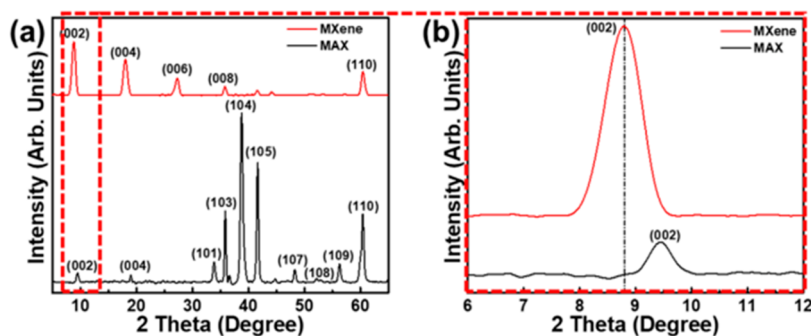


Figure 4. XRD pattern of (a) MAX powder (Ti_3AlC_2) in comparison with MXene, indicating the peak shift and (b) magnified image showing the peak shift after MXene formation. Reproduced from ref 89. Copyright 2021 American Chemical Society.

Chemical vapor deposition is a method for directly synthesizing 2D transition metal carbides, allowing for coatings via reactions on the target material. The MXene grown by the CVD method has a larger size, fewer defects and disorders, a lower concentration of impurities, and higher crystallinity than the wet chemical etching method.⁶⁸ Xu et al. reported the fabrication of a large area of high-quality 2D ultrathin $\alpha\text{-Mo}_2\text{CT}_x$ crystals by CVD at a high temperature of 1085 °C with good superconducting properties.⁷⁸

Along with the chemical vapor deposition technique, the template method is also beneficial for synthesizing MXenes with a greater output. The synthesized MXene depends on the structure of transition metal oxides, which are used to carbonize or nitridize to form MXenes.⁸ Xiao et al. synthesized MoN films by the salt-templated method, displaying a very high volumetric capacitance of 928 F/cm³ with a better rate performance in sulfuric acid electrolytes.⁷⁹ Zhang et al. experimentally demonstrated the ultrathin Mo₂C single-crystalline films by plasma-enhanced pulsed-laser deposition at 700 °C.⁸⁰

In summary, many preparation techniques have been developed, which is the result of both the diversity of carbides that can be used as raw materials and the substantial increase in demand for MXene. These techniques may narrow down the potential applications of MXene but are still in an exploratory stage. Certain challenges are associated with various MXene preparation methods; yet, they are currently under investigation to address these concerns. MXenes can be designed with high gravimetric capacitance by using different etching processes to maximize their potential for use in energy-storage applications and other areas.

4. STRUCTURE OF MXENE

MXenes are structurally similar to graphene, so they are suffixed as “enes” with high structural and electronic adaptabilities. They have accordion-like structures for high electrical conductivity, and decreasing ion diffusion distance for electron transfer shows potential in high-performance supercapacitors.⁹³ The MAX phase has a lamellar structure with M atoms that are hexagonally close-packed, X atoms filling their octahedral spaces, and the A layer acting as a mirror plane.⁵⁵ The MAX structures are anisotropic with the space group $P63/mmc$.^{94,95} The etching treatment at high temperatures removes A atoms and obtains the rock salt structure of carbide layers, similar to graphene.¹⁴ After etching A layers, 2D close-packed hexagonal structured M_{n+1}X_n layers were obtained with the terminations O, H, F, and Cl atoms.⁹⁶ Wang et al. and their co-workers documented that the titanium carbide MXene is a crystal structure through the valence electron density distribution of the particle, and its space

group is $P3m1$.⁹⁷ The XRD patterns of the MAX phase and MXene are shown in Figure 4. The distinguishing sharp peak of “Al” (104), at $2\theta = 38.8^\circ$, can be seen in Ti_3AlC_2 . This “Al” totally desires to be etched out from Ti_3AlC_2 to attain high-quality MXene with greater separation of layers. The characteristic (104) peak of “Al” in Ti_3AlC_2 almost vanished in the case of MXene by HF treatment. The morphological structure is shown in Figure 5.⁹⁸ The accordion-like morphology of MXene is

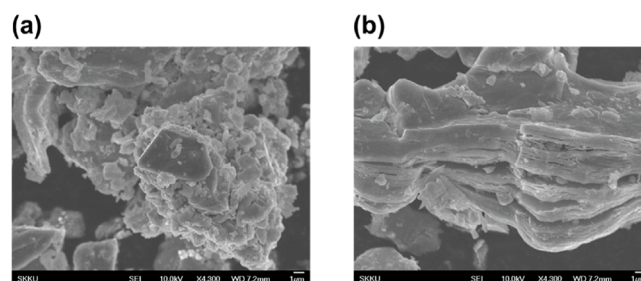


Figure 5. Scanning electron micrographs of the (a) MAX phase (Ti_3AlC_2) and (b) accordion-like structure of exfoliated MXene. Reproduced from ref 89. Copyright 2021 American Chemical Society.

obtained after the HF treatment. The surface of MXene is responsible for the energy storage mechanism. Overall, the layered structure and tunability of surface functional groups of MXene make them a versatile class of materials with the potential for numerous technological advancements.

5. PROPERTIES OF MXENE

The transition metal atoms of MXene possess abundant electrons responsible for surface interactions of MXene and are accountable for their properties. The energy bandgap and electronic conductivity of MXene depend on the surface function, which shows different applications in electronic devices based on the energy bandgap values. Khazaei et al. deliberately studied the electronic properties of M_2X with functional groups ($-\text{F}$, $-\text{OH}$, $-\text{O}$) and included that the MXenes are metallic without surface terminations.⁹⁹ To increase the conductivity of MXene, which can be made into a metal-like, semi- or full-insulating material, including the choice of M and X and the modification of their surface terminal groups.⁵ Due to variations in the surface functionalities, defect concentration, d -spacing between MXene particles, delamination yield, and lateral dimensions brought about by the etching process, the electrical conductivities of $\text{Ti}_3\text{C}_2\text{T}_x$ varied from 850 to 9870 S/m.⁷⁴ Mechanical properties influence the electrochemical properties of MXene. Gogoti et al. experimentally proved that

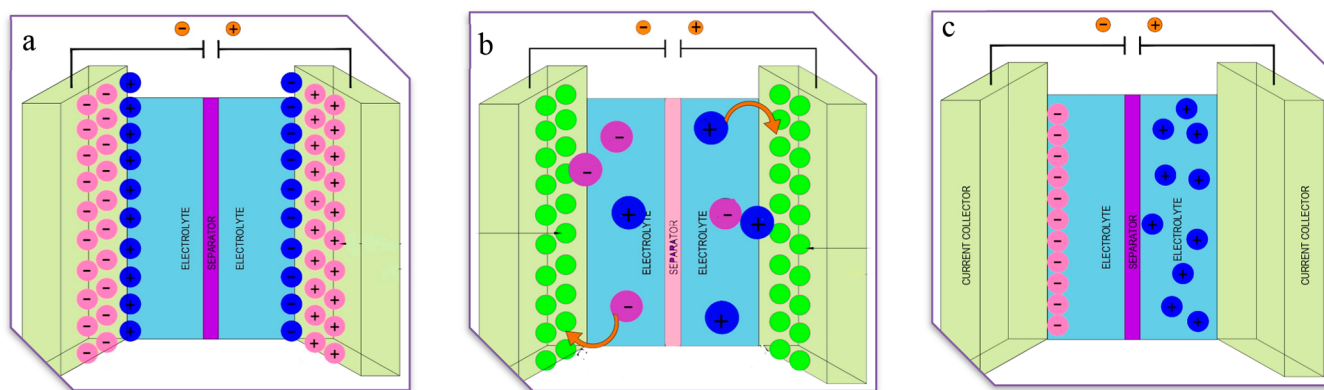


Figure 6. Diagram of (a) EDLC, (b) pseudocapacitor, and (c) hybrid capacitor.

the polymer (PVA) confinement between the MXene flakes increases flexibility and cationic intercalation with a capacitance of 530 F/cm^3 for MXene/PVA–KOH composite film at 2 mV/s . It was found that the diverse microstructures of the $\text{Ti}_3\text{C}_2\text{T}_x$ -based samples led to significant differences in their dielectric properties. Conductive and polarization loss are two types of dielectric loss; flake area and flaws disturb dielectric properties.¹⁰⁰

Temperature and environment strongly influence the MXenes' surface chemistry and phase stabilities. The specific heat, thermal conductivity, and thermal expansion coefficient control the electrochemical performance of MXene.¹⁰⁰ The introduction of heat affects the thermal properties of MXene and has led to a wide range of applications. Li et al. described that $\text{Ti}_3\text{C}_2\text{T}_x$ MXene was stable up to $800 \text{ }^\circ\text{C}$ under an argon atmosphere.¹⁰¹ Mo_2CT_x MXene is immersed in numerous solvents such as ethanol, HCl, and isopropanol and annealed in air at $200 \text{ }^\circ\text{C}$ for 2 h. Still, no significant structural changes were observed, indicating its thermal and chemical stability.¹⁰² $\text{Ti}_3\text{C}_2\text{T}_x$ MXene has thermal stability of around 108 W/mK .¹⁰³

In MXene, the transition metal's band structure and electronic transitions amid them impact its optical properties.⁸ Thin MXene-based films with outstanding optoelectronic properties, mechanical flexibility, and electric conductivity can be prepared by drying solution-processed films.²⁰ Ying et al. reported the first study on the optoelectronic properties of V_2CT_x and its processing into flexible transparent films.¹⁰⁴ The chemical stability of MXenes influences the composition, reaction conditions, and colloidal solution, which affect the applications due to their sensitivity to the outer environment. The oxidation state of the M element in MXene is much lower than the oxidation states of the termination groups. Redox oxidation can control the oxidation state, in which MXene acts as a reducing agent.^{105,106} The MXene $\text{Ti}_3\text{C}_2\text{T}_x$ synthesized from Ti_3AlC_2 shows high stability in aqueous solutions, oxidation resistance properties, and crystallinity and more significant electronic conductivity up to $20,000 \text{ S/cm}$. It can provide different methods to fabricate highly stable MXene.⁹³ Organic electrolytes can offer broader electrochemical stability than aqueous electrolytes.¹⁰⁷ Zhang et al. presented that freezing MXenes prevents the development of TiO_2 nanoparticles at the edges of the MXene flakes and holds the morphology for up to 650 days, while freshly prepared MXene displays flake edge ruining within 2 days at room temperature. The results suggested that the freezing delayed MXene oxidation.¹⁰⁸ By adjusting the stoichiometric ratios of the M and X components, it is possible

to tailor the exceptional properties of the MXene. The distinct and adaptable characteristics of MXene make them potential candidate materials for developing high-power and high-energy-density capacitors while also making them appealing for various applications. Research on MXenes is an ongoing process, and current studies are continuously revealing new properties and expanding the realm of potential applications.

6. ELECTROCHEMICAL APPLICATIONS OF MXENE

MXene attained great importance in exploring electrode materials with good electrochemical energy storage properties, excellent electrical conductivity, hydrophilic surfaces, mechanical stability, and an intercalation effect.¹⁰⁹ The unique accordion-like design decreases the ion diffusion path, and the high electrical conductivity for electron transfer shows the application of high-performance supercapacitors.⁹³ The fluoride-free etching process not only allows for a safer MXene preparation but also results in excellent electrochemical performance due to the elimination of $-\text{F}$ terminations.³ The functional group $-\text{F}$ -terminated MXenes have lower insertion–desorption potentials and a large capacity for charge storage.¹¹⁰ The intercalation method can influence the terminal surface groups, which has an effect on the electrochemical performance of MXenes.¹¹¹ The electrochemical properties of MXene strongly depend on the surface chemistry and transition metal layers. Surface groups on the MXene surface provide functionalization through covalent or noncovalent bonding.¹¹²

Chen et al. synthesized glycine-functionalized MXene with increased interlayer spacing for charge storage.¹¹³ The selection of etchant strongly influences the surface functional group, which results in the adsorption and diffusion of metal ions on the surface.¹¹⁴ The chemical etching method enables the simultaneous growth of MXenes retentive to their active surfaces for improved ion diffusion pathways, structural stability, and charge storage dynamics.¹¹⁵ The chemical action on the surface of the MXene provides capacitance. Capacitors store charges by adsorbing and desorbing electrolyte ions on the surface of electrodes.¹¹⁶

Electrostatic double-layer capacitors follow a nonfaradaic reaction because there is no charge transformation, and the energy is stored between the electrode interface and electrolyte.^{117,118} Since pseudocapacitor electrodes are made of redox-active materials, they can store energy through faradaic redox processes.⁶ The charges are transferred between the electrode and electrolyte when an external potential is applied.⁴⁷ The energy storage mechanism operates simultaneously with one as

notable as the hybrid supercapacitor, which combines non-Faradaic EDLC and a Faradaic pseudocapacitor.^{119,7} It can accept both the benefits and drawbacks of EDLC and pseudocapacitors.¹²⁰ The energy storage is either by electrostatic charge accumulation at the electrode–electrolyte interface or by charge transfer by the Faradaic reaction. It is attributed to the large surface area of electrodes and pseudocapacitor stores by fast surface redox reaction at the surface of the active materials by ion intercalation.¹²¹ Figure 6 shows the schematic representation of EDLC, pseudocapacitor, and hybrid capacitor. In an aqueous electrolyte, metal ions are combined with a water molecule to form an electric double-layer structure on the surface of MXene, and oxidation–reduction can occur to enhance capacitance. The organic electrolyte is influential in deciding the electrochemical charge storage mechanisms.¹²² The PC/Ti₃C₂ composite has efficient desolvation during charging, impacting high volumetric charge storage capacity and fast charge transport.¹²³ In nonaqueous electrolytes, significant potential differences on the surface of MXene cause the electric double-layer structure. The electrolyte can control ion transport and intercalation with interlayer spacing. MXenes with layered structures will deposit ions during cyclic charge and discharge, but their energy density may be incomplete, affecting the supercapacitor applications.¹² Ions are absorbed on the external adsorption sites at the edges of the layers and the deep adsorption sites with higher activation energy. At high scan rates, ions are rapidly adsorbed at external adsorption sites, resulting in a good rate performance of MXene. Also, the desorption of ions from deep adsorption sites at a higher voltage window results in high Faradaic efficiency and a long life cycle. The larger cations and smaller cations with higher charges expand and contract the interlayer spaces of MXene, respectively.⁸ The ionic transport medium (electrolyte), electronic transport medium (electrode), and their interfaces play a vital role in the electrochemical capacitance of supercapacitors.¹²¹ It is crucial to remember that the oxidation process primarily improves the effectiveness of ion transport. However, once the efficiency of ion transport reaches a certain point, electronic conductivity will become the dominant factor influencing the electrochemical performance of Ti₃C₂T_x. Therefore, preserving or improving Ti₃C₂T_x's electrical conductivity is essential while developing the oxidation process.¹²⁴

Flexible devices, such as flexible displays, electronic skin, human–machine interfaces, intelligent monitors, *etc.*, have demonstrated significant utility in several fields. It has significantly increased the need to develop efficient power sources for these wearable electronics. Supercapacitors must have mechanical properties compatible with human skin for use as wearable electronic power sources. It necessitates that the supercapacitors be able to provide continuous power under the varying deformations caused by human motions and be pleasant to wear. Developing solid-state supercapacitors with high mechanical flexibility has received considerable attention, but they are not yet suitable for wearable applications. Due to the rigidity of the electrodes, the freezing of the electrolyte, and problems with interfacial contact, it is still challenging to create a flexible, all-solid supercapacitor that can function under various deformations and in severe environments.⁷⁴ The microstructure of MXene can be improved by increasing its surface area and active site outcomes for the electrochemical performance. Ti₃C₂T_x has been demonstrated to be the most ideal for energy storage due to its multiple ions, faster ion diffusion, low intercalation potentials, and higher theoretical capacities.⁴⁰

The restacking of the MXene film confines the high energy density of supercapacitors. The addition of conducting polymer PEDOT and metal oxide Fe₂O₃ into MXene results in an increase in capacitance value up to 541 F/g, due to many active sites on the surface of MXene and its excellent hydrophilicity.¹²⁵ CNTs can effectively bind the restacking of MXene nanosheets, utilizing the MXene's surface active sites and enabling fast ion and electron transport.¹²⁶ The CNT in the Ti₃C₂T_x/CNT/CuS composite avoids the restacking of MXene sheets and allows large electroactive sites to become available for the electrolyte ions.⁴¹ Gandla et al. demonstrated that Mo₂Ti₂C₃ MXene with larger interlayer spacing is more beneficial in ionic liquid electrolytes than conventional Ti₃C₂T_x MXene with high specific capacitance, cycle stability, and superior energy.¹²⁷

Microsupercapacitors (mSCs) are an essential power source for portable devices. They can provide vital energy and power in a short amount of time. Optimizing and enhancing their constituent parts can alter the device's capability.⁵ The fabrication of PANI@rGO/Mxenes as electrodes for a lightweight, thin, stretchable, and wet-adhesive all-hydrogel micro-supercapacitor (mSC) and its first implantation onto the heart of living mice provided a practical application of MXene electrode-based supercapacitors.¹²⁸ Utilizing significant ion intercalation between the multilayers of MXene-based electrodes, enhanced metallic conductivity can improve the charge storage capacity quickly, thus positioning them as a prime choice for applications involving mSC electrode materials.^{77,129}

The high electrical conductivity of MXenes enables rapid charge and discharge cycles. This characteristic is beneficial when a quick energy supply is necessary, such as in power backup devices and regenerative braking systems. The electrical conductivity of MXenes makes them suitable for electromagnetic interference (EMI) shielding. MXene films with a thickness ranging from 40 nm to many micrometers show promise as thin EMI shielding coatings.¹³⁰ MXene-based electrodes can provide excellent cycle stability because of their sturdy construction and mechanical strength. Therefore, they are ideal for long-term reliable applications, including energy storage in remote locations and wearable electronics.¹³¹ MXene-based supercapacitors can be integrated with energy-harvesting technologies to store energy from sources like vibrations, light, and thermal gradient.¹³² MXenes can be combined with other substances to make hybrid supercapacitors, such as conducting polymers or transition metal oxides. These hybrids can combine the advantages of many materials, improving the performance in terms of cycling stability and energy density. These applications demonstrate the adaptability of MXenes and their potential to transform numerous sectors. It is important to remember that MXenes are still a topic of active research and that many of these fields may require additional development and optimization before they can be used practically.

7. MXENE-BASED COMPOSITES

7.1. MXene–Carbon Composites. Carbon nanomaterials such as carbon nanotubes and graphene are considered suitable materials to compound with MXene to manufacture highly flexible SCs.^{133,117} Li et al. fabricated flexible Ti₃C₂T_x MXene and electrochemically exfoliated graphene with a greater volumetric specific capacitance of 216 F/cm³ and admirable flexibility and conductivity.¹³⁴ Kumar et al. grew graphene on Ni foil and fabricated an electrode of Ti₃C₃T_x/graphene/Ni, achieving a high specific capacitance of 542 F/g at a 5 mV/s scan rate. This higher capacitance is credited to the higher

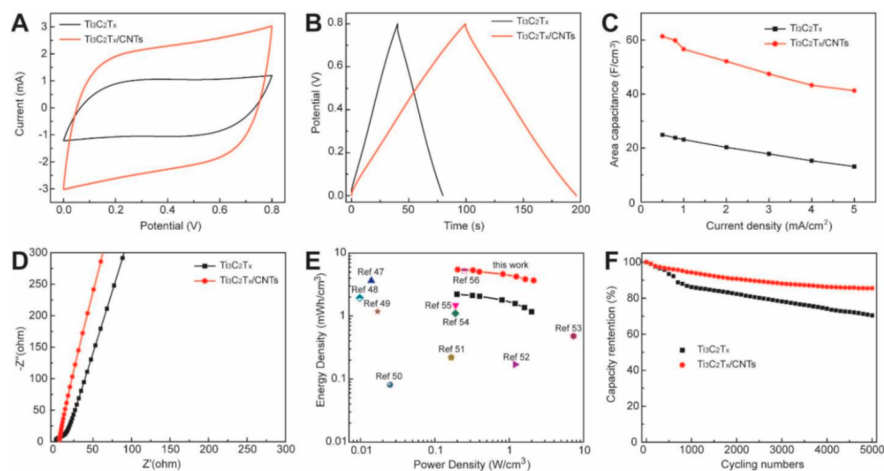


Figure 7. Electrochemical testing of $\text{Ti}_3\text{C}_2\text{T}_x$ -CNTs and $\text{Ti}_3\text{C}_2\text{T}_x$ -based single mSC devices. (A) CV curves at 10 mV/s, (B) GCD curves at 0.5 mA/cm², (C) rate capacity, (D) EIS, (E) Ragone plots, and (F) cycling stability for 5000 times. Reproduced from ref 127. Copyright 2021 American Chemical Society.

surface area, proper interlayer spacing, and intercalated faradaic reaction between MXene layers.¹³⁵ Sikdar et al. developed 3D hydrogel hybrids of MXene and graphene as suitable electrodes for pseudocapacitors, showing a high specific capacitance of 357 F/g at a 10 mV/s scan rate. The interconnected hydrogel structure of this composite keeps excellent electrical connections throughout the electrode and helps electron transfer, which is responsible for this specific capacitance value.¹³⁶ Nie et al. formulated a scalable spray-coating and dip-coating strategy to construct an rGO/MXene composite, which displays a specific capacitance of 383.3 F/g. It is attributed to the synergistic effects between rGO and MXene and the high surface area.¹³⁷ An electrolyte-mediated method is used to compound rGO/MXene composite films as self-supporting electrodes. It shows a volumetric capacitance of 454.9 F/cm³ at a high mass ratio of MXene because the electrolyte layer between rGO and MXene promotes unceasing ion transport channels in composite films.¹³⁸

CNTs are cast off to compound with an MXene because they can prevent MXene films from adhering.¹³⁹ Kim et al. and colleagues fabricated a CNT/MXene electrode of an asymmetric supercapacitor by the biscrolling method with high mass loading of MXene, which showed a suitable capacitance of 35.5 F/cm³ and increased energy and power densities of 100 μWh/cm² and 260 μWh/cm², respectively.¹⁴⁰ Luo et al. fabricated a new compact, flexible microsupercapacitor based on CNT/MXene, indicating that the interaction of electrolyte ions with $\text{Ti}_3\text{C}_2\text{T}_x$ results in the superior electrochemical performance shown in Figure 7.¹⁴¹ The triangular GCD curves at current densities ranging from 0.5 mA/cm² to 5 mA/cm² (Figure 7B) further support these capacitive behaviors. At a current density of 0.5 mA/cm², a $\text{Ti}_3\text{C}_2\text{T}_x$ -CNT-based mSC exhibits areal and volumetric capacitance of 61.38 F/cm² and 87.68 F/cm³, shown in Figure 7C. In comparison, 67.2% capacitance is retained at a high density of 5 mA/cm² (Figure 7D). The Ragone plot of the $\text{Ti}_3\text{C}_2\text{T}_x$ -CNTs and $\text{Ti}_3\text{C}_2\text{T}_x$ -based mSCs' energy density and power density is shown in Figure 7E. After 5000 charge/discharge cycles, cycling stability shows that $\text{Ti}_3\text{C}_2\text{T}_x$ -CNTs and $\text{Ti}_3\text{C}_2\text{T}_x$ -based mSCs preserve 85.5% and 70.7% of their initial capacitance, respectively (Figure 7F). MXene/CT@Ni is synthesized by exhibiting a maximum specific capacitance of 990.8 F/cm³ at 1 A/g.¹⁴² Liang et al. constructed an asymmetric

device of $\text{Ti}_3\text{C}_2\text{T}_x$ /MCNT negative electrodes and Ppy-coated MCNT positive electrodes with a reliable capacitance of 22 for the first time. Wang et al. formed a free-standing, flexible, and structurally 3D-interconnected MXene/graphyidne nanotube composite for a high-performance flexible electrode with a significantly improved capacitance of 337.4 F/g. The authors concluded that it is a novel approach to solving the stacking problem for excellent supercapacitors. The specific effects of adding carbon to MXenes depend on a variety of variables including the type of carbon used (such as graphene or carbon nanotubes), the synthesis method used, the amount of carbon added, and the intended application. Researchers delve into these factors to precisely engineer the properties of carbon-infused MXenes, tailoring them to fulfill the specific requirements of the desired functionalities. The effects include enhanced electrical conductivity, charge storage capacity, cycling stability, ion intercalation behavior, and electrocatalytic activity. This adaptability of MXenes, combined with their ability to synergize with carbon, widens the scope for creating novel materials with improved attributes, thereby offering diverse solutions for a broad spectrum of technological applications.

7.2. MXene–Metal Oxide Composites. Compared with bimetallic transition metal oxides, transition metal oxides have a higher electrical conductivity potential, a synthetic effect, and multiple valence changes. Transition metal oxides such as MnO₂, NiO, RuO₂, etc., keep an ultrahigh pseudocapacitance compared to carbon materials, which is advantageous for restructuring the low energy density and improving the cycle stability of supercapacitors.¹⁴³ The *ex situ* method is the least used to synthesize MXene–metal oxide composites among different synthesis methods. Torelli et al. prepared $\text{Ti}_3\text{C}_2\text{T}_x/\text{Co}_3\text{O}_4$ by this method.¹⁴⁴ Gong et al. successfully fabricated hexagonal nickel cobalt-oxide nanosheets on MOF and MXene composites with high specific capacitance and better cycle stability. It can afford more active sites to speed up the reaction rate of redox reactions and accelerate ion diffusion due to their hexagonal structure.¹⁴⁵ Zhu et al. and co-workers successfully synthesized the TiO_2 - $\text{Ti}_3\text{C}_2\text{T}_x$ nanocomposite through *in situ* hydrolysis and heat treatment. They fabricated it as an electrode with greater specific capacitance and ultralong cycle life. TiO_2 - $\text{Ti}_3\text{C}_2\text{T}_x$ displays a higher specific capacitance of 143 F/g at 5

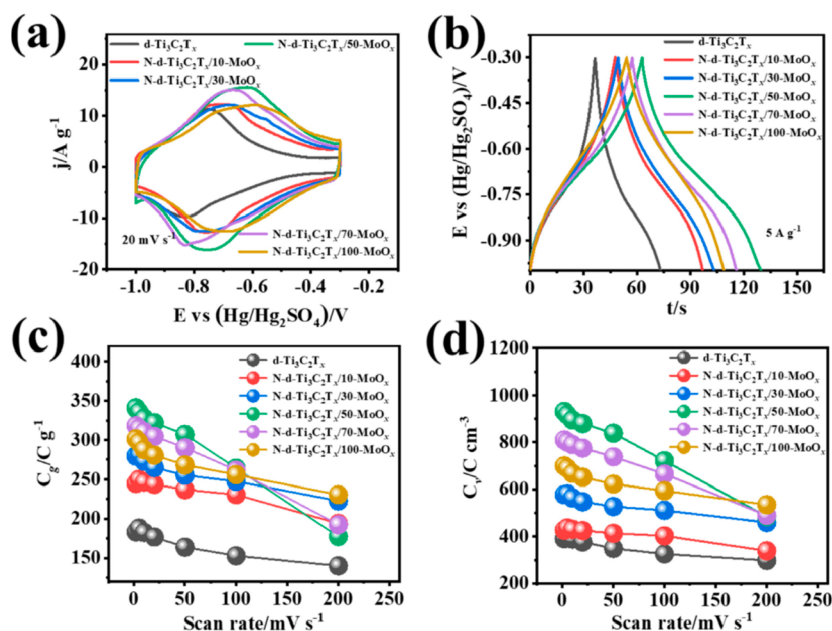


Figure 8. $D\text{-Ti}_3\text{C}_2\text{T}_x$ and $N\text{-d-Ti}_3\text{C}_2\text{T}_x/\text{MoO}_x$ films with different mass loadings of MoO_x nanoparticles: (a) CV curves at 20 mV s^{-1} , (b) GCD curves at 5 A g^{-1} , and (c,d) gravimetric and volumetric capacity at different scan rates. Reproduced from ref 140. Copyright 2021 Elsevier.

mV/s , 1.5 times that of pristine $\text{Ti}_3\text{C}_2\text{T}_x$. It is because the TiO_2 nanoparticles increase the interlayer distance of $\text{Ti}_3\text{C}_2\text{T}_x$ to enable the pull-out of cations and maintain a diffusion path for the electrolyte ions.¹⁴⁶

$\text{V}_2\text{O}_5/\text{Ti}_3\text{C}_2\text{T}_x$ is prepared by the combination of minimal delamination, vacuum-assisted filtration technique, and redox method and shows considerable cyclic stability and gravimetric capacitance.¹⁴⁷ The vacuum-assisted filtering of a mixture of MXene nanosheets and V_2O_5 nanofibers successfully produced MXene/ V_2O_5 films, contributing to the expansion and stabilization of the MXene interlayer gap, which is advantageous for charge diffusion or ion diffusion and transfer. Compared to pure MXene films, MXene/ V_2O_5 films' flexibility and electrochemical capabilities are improved. The electrode also has better specific capacitance and cycling stability.⁷⁰ Rakhi et al. reported for the first time that depositing $\epsilon\text{-MnO}_2$ whiskers on the surface of MXene to form electrodes for aqueous pseudocapacitors with increased surface area improved electrochemical performances in an aqueous electrolyte.¹⁴⁸ Zou et al. developed a self-assembly method to synthesize MXene/ $\alpha\text{-Fe}_2\text{O}_3$ having a high specific capacitance of 405.4 F/g at the current density of 2 A/g .¹⁴⁹ It is proved that TM-doped samples with MXene as a second electrode can enhance the performance of the supercapacitor.¹⁵⁰ Yuan et al. proposed a hydrothermal technique for self-assembling MXene- Co_3O_4 composites for a supercapacitor electrode. This fabricated electrode exhibits a larger gravimetric capacitance of 1081 F/g because Co_3O_4 nanoparticles avoid self-restacking and decrease the electron transport path.¹⁵¹ Ying et al. synthesized the $\text{Ti}_3\text{C}_2\text{T}_x\text{-NiO}$ composite by vacuum freeze-drying for electrodes with improved electrochemical performance.¹⁵² Co-Ni oxides were decorated on the surface of $\text{Ti}_3\text{C}_2\text{T}_x$ through the atomic layer deposition method and used as a pseudocapacitive electrode material, showing a higher specific capacitance of up to 1960 F/g with good cycle stability.¹⁵³ Bin et al. synthesized nitrogen-doped $\text{Ti}_3\text{C}_2\text{T}_x$ decorated with MoO_{3-x} ($N\text{-d-Ti}_3\text{C}_2\text{T}_x/\text{MoO}_x$) to attain high-performance flexible electrodes for supercapacitors carrying an ultrahigh capacity of 487 F/g at the current density of 5 A/g , as

shown in Figure 8.¹⁵⁴ The CV and GCD curves of the $d\text{-Ti}_3\text{C}_2\text{T}_x$ and $N\text{-d-Ti}_3\text{C}_2\text{T}_x/\text{MoO}_x$ films with various mass loadings of MoO_x nanoparticles are shown in Figure 8a,b. The $N\text{-d-Ti}_3\text{C}_2\text{T}_x/100\text{-MoO}_x$ film maintains a more stable specific capacity than the $N\text{-d-Ti}_3\text{C}_2\text{T}_x/50\text{-MoO}_x$ and $N\text{-d-Ti}_3\text{C}_2\text{T}_x/70\text{-MoO}_x$ films with increasing scan rate, as shown in Figure 8c,d with different mass loadings of MoO_x nanoparticles. Sui et al. synthesized $\text{Ti}_3\text{C}_2\text{T}_x/\text{MoO}_{3-x}$ composites with a high volumetric capacitance of 1893.2 F/cm^3 in $1 \text{ M H}_2\text{SO}_4$ electrolyte.¹⁵⁵ Pan et al. fabricated $\text{Ti}_3\text{C}_2\text{T}_x/\text{WO}_x$ on a carbon cloth by a facile electrochemical deposition method to deliver gravimetric capacitance of 164 F/g under the high mass loading of WO_x .¹⁵⁶ Darmiani et al. synthesized porous, wire-shaped $\text{Ni}(\text{OH})_2\text{-Ni-Ti}_3\text{C}_2\text{T}_x/\text{CW}$ electrodes with a high surface area for the first time. Many active sites show excellent capacitance of 1704.50 F/cm^3 due to the high conductance between active sites and CW.¹⁵⁷ It is important to note that the specific effects of incorporating metal oxides into MXenes can vary depending on factors such as the type of metal oxide, the synthesis method, the ratio of components, and the intended application. Researchers often study these factors to tailor the composite's properties of MXenes, and the functional properties of metal oxides make MXene-metal oxide composites highly versatile and valuable for a wide range of electrochemical applications.

7.3. MXene-Polymer Composites. The polymer's electrical, mechanical, and thermal properties can boost the stability of MXene flakes in MXene/polymer composites.^{158,159} The intercalation of polymers into MXene layers benefits the molecular level coupling between MXene and polymer molecules, which helps to improve the strength and flexibility of MXene/polymer composites.¹⁶⁰ Poly(vinyl alcohol) (PVA) is the best candidate among various polymers to fabricate MXene/polymer composites as electrodes because of its high solubility in water and abundance of hydroxyl groups.¹⁶⁰ Ling et al. synthesized single-layered MXene/PVA film by vacuum-assisted filtration followed by mixing the colloidal solution of $\text{Ti}_3\text{C}_2\text{T}_x$ films with PVA aqueous solution, which had enhanced tensile strength and high electronic conductivity.¹⁶¹ *In situ* polymer-

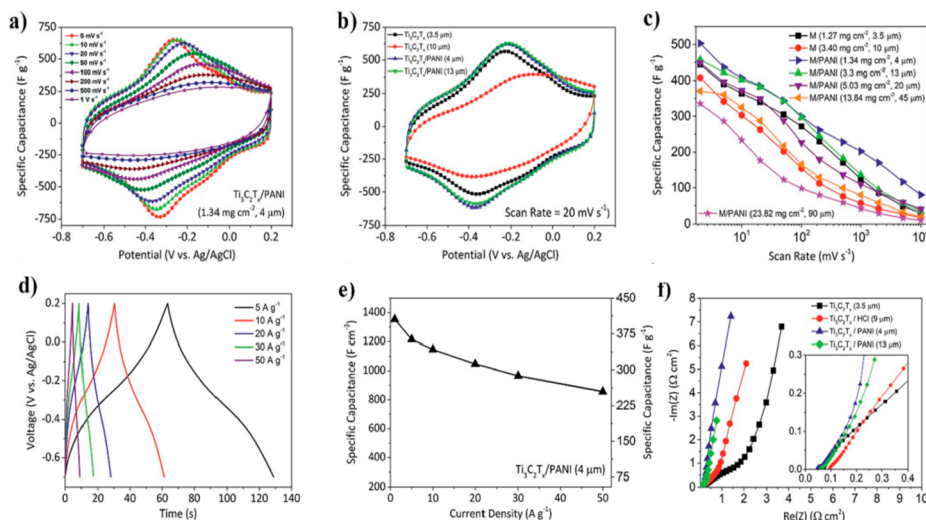


Figure 9. (a) CV curves of a $\text{Ti}_3\text{C}_2\text{T}_x/\text{PANI}$ electrode. (b) Comparison of the CV $\text{Ti}_3\text{C}_2\text{T}_x/\text{PANI}$ and $\text{Ti}_3\text{C}_2\text{T}_x$ electrodes. (c) Gravimetric capacitance of electrodes with different thicknesses and mass loadings. (d) Galvanostatic charge/discharge profiles of the $\text{Ti}_3\text{C}_2\text{T}_x/\text{PANI}$ electrode. (e) Specific capacitances of the $\text{Ti}_3\text{C}_2\text{T}_x/\text{PANI}$ electrode. (f) EIS of $\text{Ti}_3\text{C}_2\text{T}_x/\text{PANI}$ electrodes. Reproduced from ref 151. Copyright 2018 Royal Society of Chemistry.

ization and *ex situ* mixing can create MXene/polymer composites. Three processes obtain *in situ* polymerization: mild physical agitation, electrodeposition, and UV radiation, whereas the *ex situ* mixing method includes solution mixing and filtration.¹² To improve the electrochemical properties of the MXene-based electrode, Yan et al. tested the electrochemical deposition of conducting polypyrrole on the surface of the MXene electrode with a specific capacitance of 343.20 F/g.¹⁶² Naguib et al. described the synthesis and characterization of MXene/polyacrylamide (PAM) composites with greater flexibility, and conductivity increased to 3.3×10^{-2} S/m.¹⁶³ Through the intercalation of polypyrrole (PPy) into layered $\text{Ti}_3\text{C}_2\text{T}_x$ MXene, Zhu et al. found a new approach with a capacitance of about 406 F cm^{-3} . The porous structure of Ppy/ $\text{Ti}_3\text{C}_2\text{T}_x$ is the reason for excellent electrochemical output which stops the dense stacking of polypyrrole during polymerization and is advantageous to the infiltration of electrolyte into this electrode during the charging and discharging process.¹⁶⁴ Zhang et al. reported a conductive MXene/poly(3,4-ethylenedioxythiophene):polystyrenesulfonate (MXene/PEDOT:PSS) coating for an electrode in an ultrafast supercapacitor.¹⁶⁵ $\text{Ti}_3\text{C}_2\text{T}_x$ and polyaniline (PANI) hybrid electrode materials with an excellent volumetric and gravimetric capacitance of 1682 F/cm^3 and 503 F/g were created by oxidant-free *in situ* polymerization of PANI on the MXene.¹⁶⁶ The authors concluded that the PANI deposition on MXene increases the ion transport; as shown in Figure 9, the capacitance value is less thickness dependent. A freestanding $\text{Ti}_3\text{C}_2\text{T}_x/\text{PANI}$ electrode with a thickness of $4 \mu\text{m}$ and cyclic voltammetry (CV) profiles that were obtained at scan rates ranging from 5 to 1000 mV/s are displayed in Figure 9a. At a scan rate of 20 mV/s , Figure 9b contrasts the CV curves of two $\text{Ti}_3\text{C}_2\text{T}_x/\text{PANI}$ electrodes with thicknesses of 4 and $13 \mu\text{m}$ with the CV curves of two pristine $\text{Ti}_3\text{C}_2\text{T}_x$ electrodes with thicknesses of 3.5 and $10 \mu\text{m}$. The rate dependence of the gravimetric capacitance of $\text{Ti}_3\text{C}_2\text{T}_x/\text{PANI}$ electrodes with various thicknesses and mass loadings is depicted in Figure 9c. Figure 9d and e show charge–discharge profiles of the $4 \mu\text{m}$ thick $\text{Ti}_3\text{C}_2\text{T}_x/\text{PANI}$ electrode at current densities ranging from 5 to 50 A/g . The electrochemical impedance spectroscopy (EIS) results for $\text{Ti}_3\text{C}_2\text{T}_x/\text{PANI}$

electrodes of various thicknesses, a pure $\text{Ti}_3\text{C}_2\text{T}_x$ electrode, and an electrode constructed from $\text{Ti}_3\text{C}_2\text{T}_x$ crumpled by HCl treatment are shown in Figure 9f. Zheng et al. fabricated interconnected polyaniline nanoarrays and MXene networks on the fiber with high specific capacitance and energy density.¹⁶⁷ Ye et al. synthesized MXene/PANI@cotton for flexible supercapacitors with excellent electronic properties.¹⁶⁸ A flexible MXene/polymer composite with adjustable thickness presents a gravimetric capacitance of 563.8 F/g at 0.5 A/g in $1 \text{ M H}_2\text{SO}_4$.¹⁴⁷ Chang et al. used a hydrothermal method to create $\text{Ti}_3\text{C}_2\text{T}_x$ MXene with cellulose nanofiber and sodium lignosulfonate, which has a high conductivity and volumetric capacitance of 748.96 F cm^{-3} .¹⁶⁹ Table 2 summarizes the electrochemical performance of MXene–carbon composites, MXene–metal oxide composites, and MXene polymer composites. By preventing MXene sheets from being restacked and adding functionalization, the synthesis of MXene polymer composites presents a ground-breaking strategy that improves the material's electrochemical performance. Overall, the combination of MXenes with polymers creates synergistic effects that capitalize on the strengths of both materials. This hybrid approach allows for the creation of composite materials with enhanced performance, durability, and functionality, making them suitable for a wide range of electrochemical applications, including energy storage, sensors, and other electronic devices.

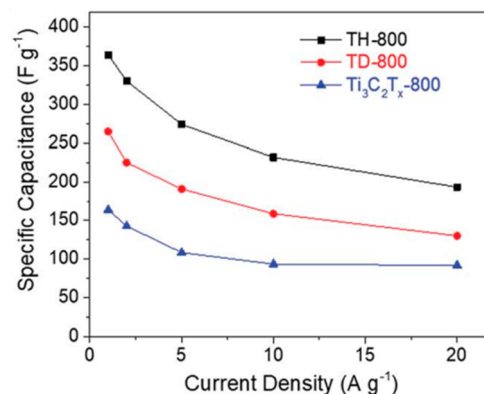
MXene-based composites are increasingly used in SC manufacturing due to their exceptional properties. MXene oxidation is close to the anodic limit of aqueous electrolytes, and proton reduction at a low voltage is restricted in symmetric supercapacitors. Combining MXene-based materials with electroactive materials that exhibit high pseudocapacitance and high operating potential in aqueous electrolytes is one method that might be used to boost the energy density of the SC device. According to these findings, a practical method for creating high-performance MXene-based composites as symmetric capacitors can be suggested, and an efficient method for enhancing the design of MXene-based electrodes is provided.

Table 2. Summary of Electrochemical Performance of Different MXene-Based Composites

	MXene-based composites	Capacitance (F/cm ³)/(F/g)	Cyclic stability (cycles)	ref
MXene–carbon composite	MXene/CNT	990.8 F/cm ³	5000 (78%)	142
	SWCNT/MXene	390 F/cm ³	10000	170
	Graphene/MXene	216 F/cm	2500 (82%)	134
	Graphdiyne/MXene	337.4 F/g	10000 (88.2%)	171
MXene–metal oxide composites	TiO ₂ /MXene	143 F/g	6000 (92%)	137
	MnO ₂ /MXene	212 F/g	10000 (88%)	148
	M-NC@NCM/NF	118.5 F/g	5000 (75.3%)	145
	Co ₃ O ₄ /MXene	1081 F/g	8000 (83%)	151
	Ti ₃ C ₂ T _x /MoO _{3-x}	733.8 F/g		155
	Fe ₂ O ₃ /MXene	405.4 F/g	2000 (97.7%)	149
MXene polymer composites	Ni(OH) ₂ –Ni–Ti ₃ C ₂ @CW	1704.5 F/cm ³	7000 (89.3%)	157
	PVA/MXene	528 F/cm ³	10000	161
	Ppy/MXene	343.20 F/cm ³		162
	Ppy/MXene	406 F/cm ³	20000 (100%)	164
	PANI	1682 F/cm ³		166

8. FACTORS INFLUENCING THE ELECTROCHEMICAL PERFORMANCE OF MXENE-BASED SUPERCAPACITORS

8.1. Dependency on the Synthesis Method. The electrochemical performance of MXene varies with the synthesis procedure. The intercalation with cations of MXene increased the interlayer spacing and the capacitance in sulfuric acid.¹⁷² The fluorine terminations, more significant Fe cations, and water intercalation among the FeF₃/HCl etchant layers can improve the electrochemical properties of the MXene electrode.¹⁷³ The hydrazine-treated material has an enhanced capacitance of 250 F/g in acidic electrolytes with an outstanding cycling stability for electrodes as thick as 75 μm. Some studies have revealed that adding materials and other heterostructures weakens the volumetric capacitance of MXene electrodes.¹⁷⁴ The specific capacitance of MXene synthesized through various rate performances of the MXene/C electrodes obtained under three different temperatures were compared, as shown in Figure 10.¹⁷⁵ The LiF/HCl etchant in H₂SO₄ solution shows greater capacitance than the HF etchant because of the intercalation of Li⁺ ions and water molecules, which avoids restacking MXene layers.¹⁷⁶ Tang et al. fabricated Ti₃C₂T_x film by concentrated H₂SO₄ etching with probe sonication to reach high electrochemical performance at high mass loadings. It indicates that reduced flake size, holes on the nanosheets, and increased interlayer spacing are three vital factors for MXenes to crack the restacking issue and attain high electrochemical performance at high rates without losing volumetric capacitance.¹⁷⁷ The electrochemical performance of Ti₃C₂T_x film is efficiently optimized after laser writing at a high capacitance of 322 F/g at 10 mV/s.¹⁷⁸ The carbon-intercalated Ti₃C₂T_x MXene (Ti₃C₂T_x/C) synthesized by annealing long-chain fatty amines to form carbon interlayers in MXene displays an increased interlayer spacing due to the amine interaction. The Ti₂C₂T_x/C

**Figure 10.** Rate performance of the TH-800, TD-800, and Ti₃C₂T_x-800 electrodes. Reproduced from ref 160. Copyright 2018 Royal Society of Chemistry.

heterostructure unveiled improved electrical conductivity and electrochemical performance with a gravimetric capacitance of 364.3 F/g.¹⁷⁵ The fractional elimination of Al can simultaneously solve the restacking issue and poor conductivity. The remaining layers provide space for ion diffusion and improve interlayer conductivity upgrades to higher capacitance.⁵⁵ In summary, the synthesis method plays a pivotal role in determining the electrochemical performance of the MXene-based supercapacitors. Researchers must carefully select or design a synthesis approach that aligns with the desired electrochemical properties and device requirements. A comprehensive understanding of how different synthesis parameters impact the resulting material properties is essential for tailoring MXene-based electrodes to achieve high-performance supercapacitors with enhanced energy and power densities.

8.2. Dependency on the MXene Precursor. Besides the synthesis method, the electrochemical properties depend on the MXene precursors. The ball milling treatments on the precursor V₄AlC₃ and HF-etched V₄C₃T_x MXene electrode in 1 M H₂SO₄ exhibited a higher capacitance of 209 F/g at a scan rate of 2 mV/s with long cyclic stability. It approved the role of the valence state of vanadium along with the greater interlayer spacing, good conductivity, and sizable porous surface of MXene.¹⁷⁹ MXene produced by two different etching protocols converted the (Mo_{2/3}Y_{1/3})₂AlC i-MAX phase into either (Mo_{2/3}Y_{1/3})₂C with in-plane elemental order after Al removal or Mo_{1.33}C with in-plane vacancy ordering after Al and Y removal. The electrochemical properties of these materials show a different result. (Mo_{2/3}Y_{1/3})₂C MXene exceeded a volumetric capacitance of 1500 F/cm³ at 2 mV/s in KOH electrolyte, and Mo_{1.33}C exceeded 1100 F/cm³ at 2 mV/s in H₂SO₄,¹⁸⁰ as is shown in Figure 11. Halim et al. noted that Mo_{1.33}C etched from the (Mo_{2/3}Sc_{1/3})₂AlC delivered a high capacitance of about 1308 F/cm³ in 1 M H₂SO₄ electrolyte, which is superior compared to (Mo_{2/3}Y_{1/3})₂AlC i-MAX phase precursors. The rate of capability improved by changing the electrolyte to 3 M H₂SO₄.⁵⁶ In conclusion, the choice of MXene precursor material significantly influences the electrochemical performance of the MXene-based supercapacitors. Careful selection of the precursor material is pivotal in determining the resulting MXene's chemical composition, layered structure, surface chemistry, and overall properties. These precursor-dependent characteristics subsequently impact the accessible surface area, pseudocapacitive behavior, conductivity, and stability of the MXene as an electrode.

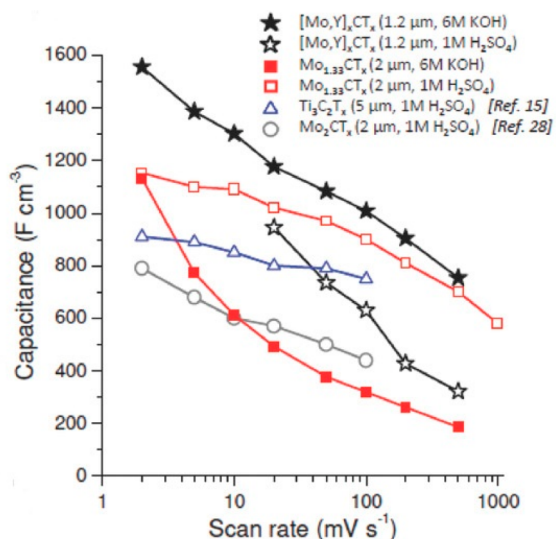


Figure 11. Scan rate dependence of volumetric capacitance of a 1.2 μm ($\text{Mo}_{2/3}\text{Y}_{(1-x)/3}\text{C}$) film and a 2 μm $\text{Mo}_{1.33}\text{C}$ film in 1 M H_2SO_4 and 6 M KOH. Reproduced from ref 165. Copyright 2018 American Chemical Society.

8.3. Dependency on the Electrolyte. The electrolyte is an essential component of supercapacitors and has attracted many concerns, and the electrochemical properties of MXene-based materials can be modified by varying electrolytes. The potential window selected by the electrolytes generates a free path for the diffusion of ions between the electrodes, and the electrolytes increase interlayer spacing by cation intercalation.¹⁸¹ Sulfuric acid is a common aqueous electrolyte; its cation is a small-sized hydrogen ion responsible for high ionic conductivity.¹⁸² The 3 M KOH alkali electrolyte of $\text{Ti}_3\text{C}_2\text{T}_x$ MXene exhibits excellent electrochemical capacitor application compared to the 3 M Na_2SO_4 neutral electrolyte.¹⁸⁵ The PAA-NHEA-MXene with an organic gel electrolyte of organic electrolyte solution (4 mol/L of LiCl/EG) is a better solid capacitor for energy storage applications.¹⁸⁴ $\text{Ti}_3\text{C}_2\text{T}_x$ MXene exhibited a high volumetric capacitance of about 1500 F/cm^3 with a 90 nm thick electrode in an acid electrolyte (1 M H_2SO_4) and the primary electrolyte (KOH), and it disclosed a volumetric capacitance of 340 F/cm^3 at 2 mV/s and exhibited almost no degradation after 10000 cycles at A/g.¹⁸⁵ Acidic- or basic-type electrolytes may leak into other parts of the system, so some gel-type electrolytes, such as poly(vinyl alcohol) (PVA/ H_2SO_4 and PVA/ H_3PO_4), are used to overcome this problem.¹⁸⁶ Most work follows acid electrolytes to accomplish high performance from MXene because of the factors contributing to its high volumetric capacitance such as its high conductivity for electron transport and its layer structures for ionic intercalation.

O-terminations for redox-active sites direct the pseudocapacitive nature of MXene in acidic electrolytes.¹⁸⁷ Fangfang et al. investigated an ionic–electronic coupling strategy for converting inactive surface functional groups into electrochemically active sites.¹⁸⁸ A reversible electrochemical reduction/oxidation is demonstrated by the anodic and cathodic peaks in the CV profile of $\text{Ti}_3\text{C}_2\text{T}_x/\text{GCE}$ which in 3 M H_2SO_4 are at -0.79 and -0.82 V with a slight potential difference of 0.03 V, respectively, as shown in Figure 12. The peak currents are 0.18 and 0.19 mA with a ratio of approximately 1. The CV curve of ($\text{Mo}_{2/3}\text{Y}_{(1-x)/3}\text{C}$) electrodes was 1.2 m thick, and the scan speeds were 20–500 mV/s in 1 M H_2SO_4 and 2–500 mV/s in 6 M KOH, as

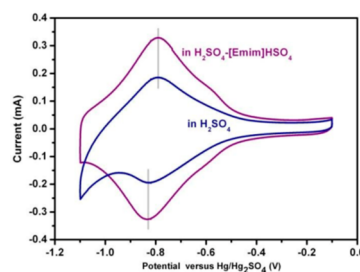


Figure 12. CVs of 1.7-IL- $\text{Ti}_3\text{C}_2\text{T}_x/\text{GCE}$ at 2 mV s^{-1} in 3 M H_2SO_4 and 3 M H_2SO_4 –0.8 M $[\text{Emim}]\text{H}_2\text{SO}_4$. Reproduced from ref 173. Copyright 2020 Royal Society of Chemistry.

shown in Figure 13.¹⁸⁰ Gogotsi et al. and co-workers experimented with different solvents to understand the effect of electrolytes on capacitance performance.¹²³ Jackel et al. tested the volume changes of $\text{Ti}_3\text{C}_2\text{T}_x$ in ionic liquid electrolytes by using the electrochemical tracing method. They verified that when the electrode attaches to electrolytes the volume expansion is irreversible due to spontaneous ion intercalation.¹⁸⁹ To sum up, the electrolyte choice holds a key role in shaping the electrochemical performance of MXene-based supercapacitors. It is imperative to comprehend how diverse electrolyte properties impact device behavior, enabling the optimization of the energy storage capacity, power delivery, and overall robustness. Therefore, researchers need to select electrolytes thoughtfully, taking into account the desired electrochemical characteristics and operational prerequisites of the supercapacitor setup.

8.4. Dependency on the Design Architecture of the Electrode. The electrochemical performance of MXene-based electrodes can be of better quality by increasing the specific surface area of the electrodes. Researchers proved that the low conductivity of transition metal oxides, the low density of carbon-based materials, and the unstable structure of conducting polymers prevent them from attaining ideal capacitance performance.^{190,191} Figure 14 shows the areal capacitance of the $\text{Ti}_3\text{C}_2\text{T}_x$ film and $\text{Ti}_3\text{C}_2\text{T}_x/\text{PDA}$ ¹⁹¹ at different scan rates. MXene-based electrodes are created by coating an MXene solution (slurry) on current collectors like Ni foam. The thickness depends on the solution concentration, which affects the supercapacitor's electrochemical performance.²⁹ The electrode's capacitance impacts its thickness; when thickness increases, the capacitance declines, which is credited to the electrode morphology.²² Lukatskaya et al. demonstrated how different electrode design strategies could push the capacitance value of MXene nearer to its theoretical value. Macroporous electrode architectures show capacitance retention of about 210 F/g at charge–discharge rates above 1 V/s and 100 F/g at 40 V/s.¹⁸⁵ Huang et al. fabricated a high-performance MXene hydrogel electrode by freezing the MXene slurry, followed by a designed thawing of sulfuric acid electrolyte, and the macrostructure of the hydrogel electrode provided plentiful active sites for the storage of ions and diffusion of the electrolyte.¹⁹² Su et al. detected that the ball milling procedure results in higher carbon content and a large electrode surface area, which upgraded the capacitance.¹⁹³ Tang et al. reported a controlled oxidation method for improving the electrochemical properties of titanium carbide MXene electrodes in acidic electrolytes by incrementally increasing the interlayer spacing and familiarizing defects without disturbing the electrochemically active sites.¹⁹⁴ In conclusion, the electrochemical proper-

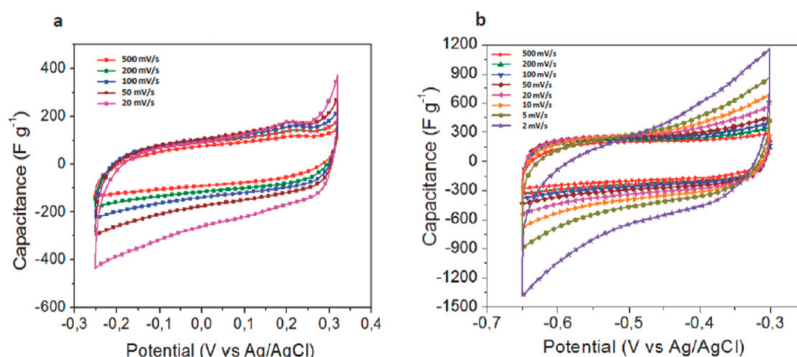


Figure 13. Electrochemical performance of a 1.2 μm thick film of $(\text{Mo}_{2/3}, \text{Y}_{(1-x)/3})_2\text{C}$: (a) 1 M H_2SO_4 and (b) 6 M KOH. Reproduced from ref 165. Copyright 2018 American Chemical Society.

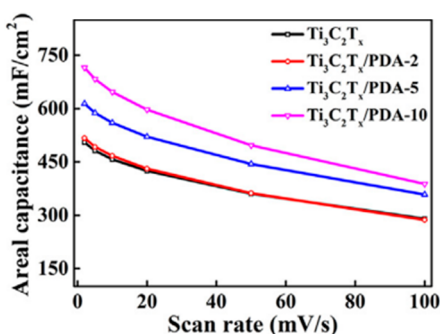


Figure 14. Areal capacitances of the $\text{Ti}_3\text{C}_2\text{T}_x$ film and $\text{Ti}_3\text{C}_2\text{T}_x/\text{PDA}$ -2, 5, and 10 composite film electrodes as a function of the scan rate. Reproduced from ref 176. Copyright 2019 Elsevier.

ties of MXene-based materials are linked to the design architecture of the electrode. Researchers must carefully engineer electrode structures to optimize the surface area, porosity, thickness, and overall configuration. A well-designed electrode contributes to the enhanced energy storage capacity, power performance, and cycling stability in various MXene-based electrochemical devices.

8.5. Dependency on the Size and Structure of MXene.

The structure and morphology affect the capacitance properties of the MXene. Structure stability has an impact on the cycling performance of a supercapacitor. Maleski et al. showed that the smaller flakes of MXene have more pathways for ions to move through. It leads to high ionic conductivity and makes it easier for the electrolyte to reach more active sites of the electrode, which increases the electrochemical performance. The larger

flake size of MXene has a minor interface contact resistance, resulting in a better electron conductivity. MXene films of about 1 μm show a larger capacitance of 288 F/g, and 4.4 μm sized films show 270 F/g.¹⁹⁵ To overcome this, Kayali et al. fabricated an electrode with a mixture of 1:1 M ratios of small flakes (below 1–2 μm) and large flakes (about $\sim 15 \mu\text{m}$) and conveyed superior gravimetric and volumetric capacitances of 435 F/g and 1513 F/cm³. A pair of anodic and cathodic peaks with tiny peak separations were seen for both electrodes at a low scan rate of 2 mV s^{-1} , and as predicted, the peaks grew wider as the scan rate was raised, as shown in Figure 15.^{196,166} Xinghua et al. experimentally proved that the ball milling of MXene can decrease particle size and enhances its electrochemical properties.¹⁹³ The size of MXene nanosheets can be controlled by fine-tuning power and the ultrasonic exfoliation time. The high ultrasonic time and power outcomes are due to the smaller size of MXene nanosheets, which positively increases active sites for ion diffusion.¹⁹⁷

Postsynthesis methods like heat treatment, intercalation, *etc.*, can alter the features of the terminal surface group. According to many studies, F-terminated $\text{Ti}_3\text{C}_2\text{T}_x$ MXene has a lower capacitance than O/OH-terminated MXene and is more susceptible to surface redox reactions because the chemical stability of $-\text{F}$ reduces electrolyte ion transfer and degrades electrochemical performance.¹⁹⁸ Surface terminations with lower electronegativity (Cl, O, F) are expected to push pseudocapacitance, and the presence of $-\text{Cl}$ increases interlayer spacing due to chlorine's large ionic size, resulting in a larger capacitance than without chloride termination.¹⁹⁹ In short, the size and structure of MXene play critical roles in determining its

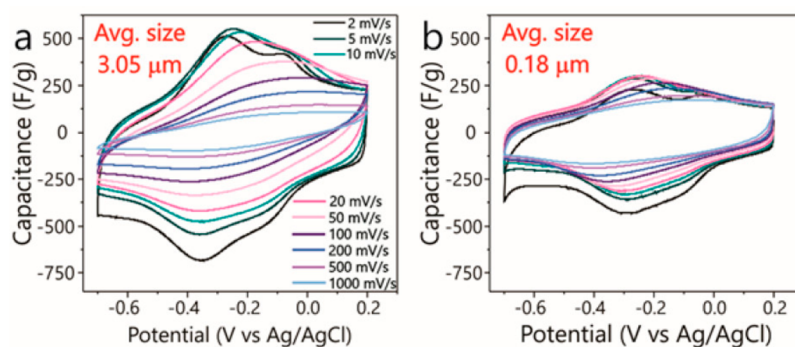


Figure 15. CV curves of (a) electrodes made using large flakes (average size of $\sim 3 \mu\text{m}$) and (b) small flakes (average size of $\sim 0.18 \mu\text{m}$). Reproduced from ref 181. Copyright 2018 American Chemical Society.

electrochemical behavior. Scientists need to carefully consider and control these factors to optimize the energy capabilities of MXene and make it more effective in various applications.

9. CONCLUSION: CHALLENGES AND FUTURE PERSPECTIVES

MXenes are promising materials for energy storage devices among 2D materials due to their unique properties. There are abundant notable studies to explore MXenes, and it has become the researchers' favorite electrode in supercapacitors. The improved properties and enhanced electrochemical performance of MXene can be used in diverse fields for energy storage applications. However, several hidden challenges delay MXene's applications in supercapacitors. Among different kinds of MXenes, Ti-based MXene is the most explored compared to other MXenes. MXenes can show higher electrochemical performance due to their properties, such as good surface chemistry, hydrophilic nature, and metallic conductivity, and the synthesis methods influence these properties. Selected etchants are used for etching A elements from the MAX phase, such as Al and Si, leading to MXenes. Surface termination groups are challenging to identify precisely using XRD and EDS. This article reviews different etching methods, but fluoride etching is still the most widely used method since it is less expensive and easier to operate than F-free. Due to fluorine surface terminations, fluoride etchants are risky and lessen the electrochemical properties, and there is a need for inexpensive, ecofriendly green etchants without sacrificing their quality. The fluorine-free etching methods simplify the effect of the pressure and temperature on the preparation of MXene. The molten salt etching method is the best method for MXene preparation and has the same features and applicability as the HF method. By an increase in the lateral size of MXene and its interlayer structure by intercalation caused by etchants, more ions can pass through it, and more faradaic charges can be stored. This type of delamination occurs without the application of a delamination agent.

Investigating novel MXene preparation methods requires significant research and is both crucial and challenging. It is necessary to develop safe, effective, and high-quality synthesis methods. The main obstacles to the production of MXene are the cost and availability of MAX phase powders and the usage of a significant amount of intrinsically dangerous high-concentration HF. These issues will continue to be barriers to the growth of the industry. The etching of MXene is time-consuming and cannot achieve mass production, which is challenging. There is a poor understanding of the surface termination effect on the MXenes' functional characteristics. It is a complex task that needs careful thought to functionalize MXene surfaces with particular groups while preserving stability and preventing degradation. Surface flaws in MXene caused by chemical etching are related to the oxidation of MXene. The aggregation of the synthesized MXene and the effects of the structural features of MXenes, such as basal spacing, surface chemistry, *etc.*, have significantly impacted the electrochemical charge storage mechanism of MXene-based electrode materials. Many MAX phases and precursors are theoretically proven through computation; however, preparation methods and studies are not explored, and experimental evidence is still necessary. Only a few reports are found on nitride-based MXene, leaving it to be barely studied.

Aqueous solutions of HF are used to synthesize nitride-based MXene, and it is imperative to design a synthesis method for

nitride-based MXene. To encourage commercialization, consider safer fabrication methods without compromising the quality or controlling the interaction of exfoliated MXene nanosheets with different solvents. It is still challenging to manufacture high-quality MXenes on a wide scale while keeping their stable characteristics. For practical applications, scalability without sacrificing the material's characteristics is essential. The diversity of MXene would be more prosperous.

MXenes with high energy and power density are very important, and MXene-based composite materials enhance the electrochemical capacitance as electrodes in a supercapacitor. The transition-metal-oxide–MXene composite is the best combination for high electrochemical properties because the porous structure with a large surface area contributes to the fast faradaic reaction. Since most polymers are hydrophobic, incorporating MXene into the polymer is a challenge faced by research. So, developing a suitable method for comprising MXene and hydrophobic polymer will benefit novel applications in the future. MXenes have been used in composites, coatings, and other sectors; thus, it is crucial to comprehend and optimize their mechanical and thermal properties. Attaining the desired thermal conductivity, stability, and mechanical strength under various conditions is an ongoing challenge. It is crucial to guarantee the long-term stability of MXenes, especially in practical applications and in diverse settings. It is still challenging to stop oxidation, degradation, or other undesirable changes from happening over time.

Aqueous electrolytes increase ionic conductivity, but in some cases, the leakage of aqueous electrolytes has an unfavorable effect on the device's electrochemical performance. Also, dissolved oxygen in the aqueous electrolyte hinders the electrochemical capacitance by surface oxidation. Hence, reports are needed for solid and nonaqueous electrolytes to achieve high electrochemical performance. Transparent and highly flexible electrodes are crucial for the next generation, and MXene looks to have a vast potential for this. It will upgrade the quality of the MXene research field to the next level. The goal of this review is to contribute favorably to the development of MXene-based electrodes for supercapacitors.

■ AUTHOR INFORMATION

Corresponding Author

Xavier Thankappan Suryabai – Centre for Advanced Materials Research, Department of Physics, Government College for Women, University of Kerala, Thiruvananthapuram, Kerala 695014, India; Email: xavierkattukulam@gmail.com

Authors

Anu Mini Aravind – Centre for Advanced Materials Research, Department of Physics, Government College for Women, University of Kerala, Thiruvananthapuram, Kerala 695014, India

Merin Tomy – Centre for Advanced Materials Research, Department of Physics, Government College for Women, University of Kerala, Thiruvananthapuram, Kerala 695014, India

Anupama Kuttapan – St Thomas College (Autonomous), Thrissur, Kerala 68001, India

Ann Mary Kakkassery Aipponny – St Thomas College (Autonomous), Thrissur, Kerala 68001, India

Complete contact information is available at:

<https://pubs.acs.org/10.1021/acsomega.3c02002>

Author Contributions

Anu Mini Aravind: Data collection, Writing—review and editing. Merin Tomy: Review and editing. Anupama Kuttapan: Review and editing. Ann Mary Kakkassery Aippunny: Coordination, review, and editing. Xavier Thankappan Suryabai: Conceptualization, supervision, review, and editing.

Notes

The authors declare no competing financial interest.

Biographies

Anu Mini Aravind is a physics Ph.D. student under Dr. Xavier Thankappan Suryabai at the Government College for Women, University of Kerala, Thiruvananthapuram. She received her M.Phil. in physics from the University of Kerala in 2021. Currently, her activity research is focused on the field of energy storage.

Merin Tomy graduated with a Master's degree in physics from Mahatma Gandhi University in 2018. Currently, she is a doctoral candidate in material science at the Government College for Women, University of Kerala, Thiruvananthapuram, under the direction of Dr. Xavier Thankappan Suryabai. Her research focuses on the field of energy storage.

Anupama Kuttapan is a postgraduate from St. Thomas College (Autonomous), Thrissur, in 2017. Currently, she is a research scholar in the Department of Physics at St. Thomas College (Autonomous), Thrissur, under the guidance of Dr. Ann Mary K. A. Her research primarily focuses on the optical and electrochemical analysis of specific selenium-based nanocomposites.

Dr. Ann Mary K. A. is an Assistant Professor & Research Supervisor in the Department of Physics, St. Thomas College (Autonomous), Thrissur, University of Calicut. She obtained her Master's degree in physics from Mahatma Gandhi University Kottayam in 2010 and received her Ph.D. in 2015 from the same university. Her research interests include material science, especially carbon-based quantum materials, biophotonics, nonlinear optics, and electrochemical energy storage studies. She has more than 20 publications in these areas to her credit.

Xavier Thankappan Suryabai is an assistant professor of physics at the University of Kerala, Thiruvananthapuram. He graduated in physics from Madurai Kamaraj University, Tamil Nadu, and received his Ph.D. in physics in 2011 from the University of Kerala, Thiruvananthapuram. His research is focused on density functional studies of materials. His research interests include nanomaterials, drug design, energy materials, spectroscopy, and physics education. He has published more than 35 scientific articles on these topics.

ACKNOWLEDGMENTS

We thankfully acknowledge the University of Kerala for its financial support. We also thank the Centralized Common Instrumentation Centre (CCIF), Kerala Government Project Performance Linked Encouragement for Academic Studies (PLEASE), and Government College for Women, Thiruvananthapuram, Kerala, India, DST-FIST, for executing this work.

REFERENCES

- (1) Gu, T.-H.; Kwon, N. H.; Lee, K.-G.; Jin, X.; Hwang, S.-J. 2D Inorganic Nanosheets as Versatile Building Blocks for Hybrid Electrode Materials for Supercapacitor. *Coord. Chem. Rev.* **2020**, *421*, 213439.
- (2) Zhu, Y.; Zheng, S.; Qin, J.; Ma, J.; Das, P.; Zhou, F.; Wu, Z. S. 2.4 V Ultrahigh-Voltage Aqueous MXene-Based Asymmetric Micro-Supercapacitors with High Volumetric Energy Density toward a Self-Sufficient Integrated Microsystem. *Fundam. Res.* **2022**, DOI: 10.1016/j.fmr.2022.03.021.
- (3) Zhu, Q.; Li, J.; Simon, P.; Xu, B. Two-Dimensional MXenes for Electrochemical Capacitor Applications: Progress, Challenges and Perspectives. *Energy Storage Mater.* **2021**, *35*, 630–660.
- (4) Liu, S.; Kang, L.; Jun, S. C. Challenges and Strategies toward Cathode Materials for Rechargeable Potassium-Ion Batteries. *Adv. Mater.* **2021**, *33* (47), 1–40.
- (5) Kamarulazam, F.; Bashir, S.; Ramesh, S.; Ramesh, K. Emerging Trends towards MXene-Based Electrolytes for Electrochemical Applications. *Materials Science and Engineering B* **2023**, *290*, 116355.
- (6) Thiagarajan, K.; Balaji, D.; Madhavan, J. Cost-Effective Synthesis of Efficient CoWO₄/Ni Nanocomposite Electrode Material for Supercapacitor Applications. *Nanomaterials* **2020**, *10*, 2195.
- (7) Theerthagiri, J.; Senthil, R. A.; Nithyadharseni, P.; Lee, S. J.; Durai, G.; Kuppusami, P.; Madhavan, J.; Choi, M. Y. Recent Progress and Emerging Challenges of Transition Metal Sulfides Based Composite Electrodes for Electrochemical Supercapacitive Energy Storage. *Ceram. Int.* **2020**, *46* (10), 14317–14345.
- (8) Panda, S.; Deshmukh, K.; Khadheer Pasha, S. K.; Theerthagiri, J.; Manickam, S.; Choi, M. Y. MXene Based Emerging Materials for Supercapacitor Applications: Recent Advances, Challenges, and Future Perspectives. *Coord. Chem. Rev.* **2022**, *462*, 214518.
- (9) Gu, T. H.; Kwon, N. H.; Lee, K. G.; Jin, X.; Hwang, S. J. 2D Inorganic Nanosheets as Versatile Building Blocks for Hybrid Electrode Materials for Supercapacitor. *Coord. Chem. Rev.* **2020**, *421*, 213439.
- (10) Venkateshalu, S.; Grace, A. N. MXenes—A New Class of 2D Layered Materials: Synthesis, Properties, Applications as Supercapacitor Electrode and Beyond. *Appl. Mater. Today* **2020**, *18*, 100509.
- (11) Liu, X.; Xu, F.; Li, Z.; Liu, Z.; Yang, W.; Zhang, Y.; Fan, H.; Yang, H. Y. Design Strategy for MXene and Metal Chalcogenides/Oxides Hybrids for Supercapacitors, Secondary Batteries and Electro/Photocatalysis. *Coord. Chem. Rev.* **2022**, *464*, 214544.
- (12) Yang, J.; Bao, W.; Jaumaux, P.; Zhang, S.; Wang, C.; Wang, G. MXene-Based Composites: Synthesis and Applications in Rechargeable Batteries and Supercapacitors. *Adv. Materials Inter* **2019**, *6*, 1–32.
- (13) Tomy, M.; Rajappan, A. A.; Suryabai, X. T. Emergence of Novel 2D Materials for High-Performance Supercapacitor Electrode Applications: A Brief Review. *Energy Fuels* **2021**, *35*, 19881–19900.
- (14) Anasori, B.; Lukatskaya, M. R.; Gogotsi, Y. 2D Metal Carbides and Nitrides (MXenes) for Energy Storage. *Nat. Rev. Mater.* **2017**, DOI: 10.1038/natrevmats.2016.98.
- (15) Naguib, M.; Come, J.; Dyatkin, B.; Presser, V.; Taberna, P. L.; Simon, P.; Barsoum, M. W.; Gogotsi, Y. MXene: A Promising Transition Metal Carbide Anode for Lithium-Ion Batteries. *Electrochem. Commun.* **2012**, *16* (1), 61–64.
- (16) Inman, A.; Hryhorchuk, T.; Bi, L.; Wang, R.; Greenspan, B.; Tabb, T.; Gallo, E. M.; VahidMohammadi, A.; Dion, G.; Danielescu, A.; Gogotsi, Y. Wearable Energy Storage with MXene Textile Supercapacitors for Real World Use. *J. Mater. Chem. A* **2023**, *11* (7), 3514–3523.
- (17) Gogotsi, Y. Monolithic Integrated MXene Supercapacitors May Power Future Electronics. *Natl. Sci. Rev.* **2023**, *10* (3), 5–6.
- (18) Abdah, M. A. A. M.; Awan, H. T. A.; Mehar, M.; Mustafa, M. N.; Walvekar, R.; Alam, M. W.; Khalid, M.; Umapathi, R.; Chaudhary, V. Advancements in MXene-Polymer Composites for High-Performance Supercapacitor Applications. *J. Energy Storage* **2023**, *63* (March), 106942.
- (19) Tang, J.; Huang, X.; Qiu, T.; Peng, X.; Wu, T.; Wang, L.; Luo, B.; Wang, L. Interlayer Space Engineering of MXenes for Electrochemical Energy Storage Applications. *Chemistry A European J* **2021**, *27*, 1921.
- (20) Baig, M. M.; Gul, I. H.; Baig, S. M.; Shahzad, F. 2D MXenes: Synthesis, Properties, and Electrochemical Energy Storage for Supercapacitors - A Review. *J. Electroanal. Chem.* **2022**, *904*, 115920.
- (21) Wang, Y.; Wang, Y. Recent Progress in MXene Layers Materials for Supercapacitors: High-performance Electrodes. *SmartMat* **2023**, DOI: 10.1002/smm2.1130.
- (22) Ghidui, M.; Lukatskaya, M. R.; Zhao, M. Q.; Gogotsi, Y.; Barsoum, M. W. Conductive Two-Dimensional Titanium Carbide

- “clay” with High Volumetric Capacitance. *Nature* **2014**, *516* (7529), 78–81.
- (23) Zhu, Y.; Rajouâ, K.; Le Vot, S.; Fontaine, O.; Simon, P.; Favier, F. Modifications of MXene Layers for Supercapacitors. *Nano Energy* **2020**, *73*, 104734.
- (24) Shao, H.; Xu, K.; Wu, Y. C.; Iadecola, A.; Liu, L.; Ma, H.; Qu, L.; Raymundo-Piñero, E.; Zhu, J.; Lin, Z.; Taberna, P. L.; Simon, P. Unraveling the Charge Storage Mechanism of Ti₃C₂T_x MXene Electrode in Acidic Electrolyte. *ACS Energy Lett.* **2020**, *5* (9), 2873–2880.
- (25) Shi, B.; Li, L.; Chen, A.; Jen, T. C.; Liu, X.; Shen, G. Continuous Fabrication of Ti₃C₂T_x MXene-Based Braided Coaxial Zinc-Ion Hybrid Supercapacitors with Improved Performance. *Nano-Micro Lett.* **2022**, DOI: 10.1007/s40820-021-00757-6.
- (26) Zhao, Z.; Wu, X.; Luo, C.; Wang, Y.; Chen, W. Rational Design of Ti₃C₂Cl₂MXenes Nanodots-Interspersed MXene@NiAl-Layered Double Hydroxides for Enhanced Pseudocapacitor Storage. *J. Colloid Interface Sci.* **2022**, *609*, 393–402.
- (27) Feng, C.; Jia, B.; Wang, H.; Wang, Y.; Wu, X. A Novel Strategy for High Energy Density Supercapacitors: Formation of Cyanuric Acid between Ti₃C₂T_x (MXene) Interlayer Hybrid Electrodes. *Chem. Eng. J.* **2023**, *465* (March), 142935.
- (28) Zhang, P.; Li, J.; Yang, D.; Soomro, R. A.; Xu, B. Flexible Carbon Dots-Intercalated MXene Film Electrode with Outstanding Volumetric Performance for Supercapacitors. *Adv. Funct. Mater.* **2023**, DOI: 10.1002/adfm.202209918.
- (29) Liang, W.; Zhitomirsky, I. MXene-Carbon Nanotube Composite Electrodes for High Active Mass Asymmetric Supercapacitors. *J. Mater. Chem. A* **2021**, *9* (16), 10335–10344.
- (30) Ma, F.; Li, L.; Jia, C.; He, X.; Li, Q.; Sun, J.; Jiang, R.; Lei, Z.; Liu, Z.-H. All-Solid-State Ti₃C₂T_x Neutral Symmetric Fiber Supercapacitors with High Energy Density and Wide Temperature Range. *Journal of Colloid and Interface Science* **2023**, *643*, 92–101.
- (31) Liu, R.; Zhang, A.; Tang, J.; Tian, J.; Huang, W.; Cai, J.; Barrow, C.; Yang, W.; Liu, J. Fabrication of Cobaltic Oxide Nanoparticle-Doped 3D MXene/Graphene Hybrid Porous Aerogels for All-Solid-State Supercapacitors. *Chem. - A Eur. J.* **2019**, *25* (21), 5547–5554.
- (32) Patra, A.; Mane, P.; Polaki, S. R.; Chakraborty, B.; Rout, C. S. Enhanced Charge Storage Performance of MXene Based All-Solid-State Supercapacitor with Vertical Graphene Arrays as the Current Collector. *J. Energy Storage* **2022**, *54* (April), 105355.
- (33) Zhan, X.; Si, C.; Zhou, J.; Sun, Z. MXene and MXene-Based Composites: Synthesis, Properties and Environment-Related Applications. *Nanoscale Horizons* **2020**, *5* (2), 235–258.
- (34) Zhang, Y.; Lu, W.; Zhou, J.; Sun, D.; Li, H. Facile Self-Assembly of Sandwich-like MXene V₂CT_x Ag_rGO_rMWCNTs Layered Multiscale Structure Nanocomposite. *Ceramics International* **2023**, *49*, 1911.
- (35) Kim, J.; Ryu, J. H.; Jang, M.; Park, S.; Kim, M.; Lee, K. H.; Choi, S.; Yoon, Y.; Jung, H. K.; Lee, S. S.; An, K. S. One-Dimensional π -d Conjugated Coordination Polymer Intercalated MXene Compound for High-Performance Supercapacitor Electrode. *Small Methods*. **2023**, DOI: 10.1002/smt.202201539.
- (36) Luo, W.; Sun, Y.; Han, Y.; Ding, J.; Li, T.; Hou, C.; Ma, Y. Flexible Ti₃C₂T_x MXene_{polypyrrole} Composite Films for High-Performance All-Solid Asymmetric Supercapacitors. *Electrochimica Acta* **2023**, *441*, 141818.
- (37) Yuan, T.; Zhang, Z.; Liu, Q.; Liu, X.; Miao, Y.; Yao, C. MXene (Ti₃C₂T_x)/ Cellulose Nanofiber/Polyaniline Film as a Highly Conductive and Flexible Electrode Material for Supercapacitors. *Carbohydrate Polymers* **2023**, *304*, 120519.
- (38) Gong, S.; Zhao, F.; Zhang, Y.; Xu, H.; Li, M.; Qi, J.; Wang, H.; Wang, Z.; Hu, Y.; Fan, X.; Peng, W.; Li, C.; Liu, J. Few-Layered Ti₃C₂T_x MXene Synthesized via Water-Free Etching toward High-Performance Supercapacitors. *J. Colloid Interface Sci.* **2023**, *632*, 216–222.
- (39) Pathak, M.; Polaki, S. R.; Rout, C. S. High Performance Asymmetric Supercapacitors Based on Ti₃C₂T_x MXene and Electrodeposited Spinell NiCo₂S₄ Nanostructures. *RSC Adv.* **2022**, *12* (17), 10788–10799.
- (40) Aghamohammadi, H.; Eslami-Farsani, R.; Castillo-Martinez, E. Recent Trends in the Development of MXenes and MXene-Based Composites as Anode Materials for Li-Ion Batteries. *J. Energy Storage* **2022**, *47*, 103572.
- (41) Dang, A.; Sun, Y.; Liu, Y.; Xia, Y.; Liu, X.; Gao, Y.; Wu, S.; Li, T.; Zada, A.; Ye, F. Flexible Ti₃C₂T_x/Carbon Nanotubes/CuS Film Electrodes Based on a Dual-Structural Design for High-Performance All-Solid-State Supercapacitors. *ACS Appl. Energy Mater.* **2022**, *5* (7), 9158–9172.
- (42) Zhang, C.; Ma, Y.; Zhang, X.; Abdolhosseinzadeh, S.; Sheng, H.; Lan, W.; Pakdel, A.; Heier, J.; Nuesch, F. Two-Dimensional Transition Metal Carbides and Nitrides (MXenes): Synthesis, Properties, and Electrochemical Energy Storage Applications. *Energy & Environ. Materials* **2020**, *3*, 29.
- (43) Xiong, D.; Shi, Y.; Yang, H. Y. Rational Design of MXene-Based Films for Energy Storage: Progress, Prospects. *Mater. Today* **2021**, *46* (June), 183–211.
- (44) Srinivasan, S.; Jothibas, M.; Nesakumar, N. Enhancing Electric Double Layer Capacitance of Two-Dimensional Titanium Carbide (MXene) with Facile Synthesis and Accentuated Properties. *Energy Fuels* **2022**, *36* (5), 2811–2820.
- (45) Hu, M.; Hu, T.; Li, Z.; Yang, Y.; Cheng, R.; Yang, J.; Cui, C.; Wang, X. Surface Functional Groups and Interlayer Water Determine the Electrochemical Capacitance of Ti₃C₂T_x MXene. *ACS Nano* **2018**, *12* (4), 3578–3586.
- (46) Naguib, M.; Mashtalir, O.; Carle, J.; Presser, V.; Lu, J.; Hultman, L.; Gogotsi, Y.; Barsoum, M. W. Two-Dimensional Transition Metal Carbides. *ACS Nano* **2012**, *6* (2), 1322–1331.
- (47) Tang, H.; Hu, Q.; Zheng, M.; Chi, Y.; Qin, X.; Pang, H.; Xu, Q. Progress in Natural Science: Materials International MXene - 2D Layered Electrode Materials for Energy Storage. *Prog. Nat. Sci. Mater. Int.* **2018**, *28* (2), 133–147.
- (48) Kshetri, T.; Tran, D. T.; Le, H. T.; Nguyen, D. C.; Hoa, H. V.; Kim, N. H.; Lee, J. H. Recent Advances in MXene-Based Nanocomposites for Electrochemical Energy Storage Applications. *Prog. Mater. Sci.* **2021**, *117*, 100733.
- (49) Naguib, M.; Gogotsi, Y. Synthesis of Two-Dimensional Materials by Selective Extraction. *Acc. Chem. Res.* **2015**, *48* (1), 128–135.
- (50) Raghavendra, K. V. G.; Vinoth, R.; Zeb, K.; Muralee Gopi, C. V.V.; Sambasivam, S.; Kummara, M. R.; Obaidat, I. M.; Kim, H. J. An Intuitive Review of Supercapacitors with Recent Progress and Novel Device Applications. *J. Energy Storage* **2020**, *31*, 101652.
- (51) Kumar, J. A.; Prakash, P.; Krithiga, T.; Amarnath, D. J.; Premkumar, J.; Rajamohan, N.; Vasseghian, Y.; Saravanan, P.; Rajasimman, M. Methods of Synthesis, Characteristics, and Environmental Applications of MXene: A Comprehensive Review. *Chemosphere* **2022**, *286* (P1), 131607.
- (52) Zhang, C.; Ma, Y.; Zhang, X.; Abdolhosseinzadeh, S.; Sheng, H.; Lan, W.; Pakdel, A.; Heier, J.; Nuesch, F. Two-Dimensional Transition Metal Carbides and Nitrides (MXenes): Synthesis, Properties, and Electrochemical Energy Storage Applications. *Energy & Environ. Materials* **2020**, *3*, 29–55.
- (53) Li, Q.; Li, Y.; Zeng, W. Preparation and Application of 2D MXene-Based Gas Sensors: A Review. *Chemosensors* **2021**, *9*, 225.
- (54) Kim, Y. J.; Kim, S. J.; Seo, D.; Chae, Y.; Anayee, M.; Lee, Y.; Gogotsi, Y.; Ahn, C. W.; Jung, H. T. Etching Mechanism of Monoatomic Aluminum Layers during MXene Synthesis. *Chem. Mater.* **2021**, *33* (16), 6346–6355.
- (55) Hu, M.; Zhang, H.; Hu, T.; Fan, B.; Wang, X.; Li, Z. Emerging 2D MXenes for Supercapacitors: Status, Challenges and Prospects. *Chem. Soc. Rev.* **2020**, *49* (18), 6666–6693.
- (56) Halim, J.; Etman, A. S.; Elskova, A.; Polcik, P.; Palisaitis, J.; Barsoum, M. W.; Persson, P. O. Å.; Rosen, J. Tailored Synthesis Approach of (Mo₂/3Y₁/3)2AlC: I-MAX and Its Two-Dimensional Derivative Mo_{1.33}CT_zMXene: Enhancing the Yield, Quality, and Performance in Supercapacitor Applications. *Nanoscale* **2021**, *13* (1), 311–319.

- (57) Aslam, M. K.; Xu, M. A Mini-Review: MXene Composites for Sodium/Potassium-Ion Batteries. *Nanoscale* **2020**, *12* (30), 15993–16007.
- (58) Echols, I. J.; Yun, J.; Cao, H.; Thakur, R. M.; Sarmah, A.; Tan, Z.; Littleton, R.; Radovic, M.; Green, M. J.; Lutkenhaus, J. L. Conformal Layer-by-Layer Assembly of Ti₃C₂T_x MXene-Only Thin Films for Optoelectronics and Energy Storage. *Chem. Mater.* **2022**, *34* (11), 4884–4895.
- (59) Ma, R.; Zhang, X.; Zhuo, J.; Cao, L.; Song, Y.; Yin, Y.; Wang, X.; Yang, G.; Yi, F. Self-Supporting, Binder-Free, and Flexible Ti₃C₂T_xMXene-Based Supercapacitor Electrode with Improved Electrochemical Performance. *ACS Nano* **2022**, *16* (6), 9713–9727.
- (60) Wei, Y.; Zhang, P.; Soomro, R. A.; Zhu, Q.; Xu, B. Advances in the Synthesis of 2D MXenes. *Adv. Mater.* **2021**, *33* (39), 1–30.
- (61) Prenger, K.; Sun, Y.; Ganeshan, K.; Al-Temimy, A.; Liang, K.; Dun, C.; Urban, J. J.; Xiao, J.; Petit, T.; Van Duin, A. C. T.; Jiang, D. E.; Naguib, M. Metal Cation Pre-Intercalated Ti₃C₂T_xMXene as Ultra-High Areal Capacitance Electrodes for Aqueous Supercapacitors. *ACS Appl. Energy Mater.* **2022**, *5* (8), 9373–9382.
- (62) Zhang, X.; Liu, X.; Feng, Y.; Qiu, S.; Shao, Y.; Liao, Q.; Li, H.; Liu, Y. In Situ Modified Mesoporous MXene Film with Excellent Oxidation Resistance for High-Performance Supercapacitor. *Appl. Mater. Today* **2022**, *27*, 101483.
- (63) Sun, L.; Fu, Q.; Pan, C. Hierarchical Porous “Skin/Skeleton”-like MXene/Biomass Derived Carbon Fibers Heterostructure for Self-Supporting, Flexible All Solid-State Supercapacitors. *J. Hazard. Mater.* **2021**, *410*, 124565.
- (64) Liu, F.; Wang, C.; Wang, L.; Huang, F.; Fan, J.; Shi, N.; Han, M.; Dai, Z. Oxygen-Vacancy-Rich NiMnZn-Layered Double Hydroxide Nanosheets Married with Mo₂CT_xMXene for High-Efficiency All-Solid-State Hybrid Supercapacitors. *ACS Appl. Energy Mater.* **2022**, *5* (3), 3346–3358.
- (65) Ghidiu, M.; Naguib, M.; Shi, C.; Mashtalir, O.; Pan, L. M.; Zhang, B.; Yang, J.; Gogotsi, Y.; Billinge, S. J. L.; Barsoum, M. W. Synthesis and Characterization of Two-Dimensional Nb₄C₃ (MXene). *Chem. Commun.* **2014**, *50* (67), 9517–9520.
- (66) Li, T.; Yao, L.; Liu, Q.; Gu, J.; Luo, R.; Li, J.; Yan, X.; Wang, W.; Liu, P.; Chen, B.; Zhang, W.; Abbas, W.; Naz, R.; Zhang, D. Fluorine-Free Synthesis of High-Purity Ti₃C₂T_x (T = OH, O) via Alkali Treatment. *Angew. Chemie - Int. Ed.* **2018**, *57* (21), 6115–6119.
- (67) Zamhuri, A.; Lim, G. P.; Ma, N. L.; Tee, K. S.; Soon, C. F. MXene in the Lens of Biomedical Engineering: Synthesis, Applications and Future Outlook. *Biomed. Eng. Online* **2021**, *20* (1), 1–24.
- (68) Luo, J.; Matios, E.; Wang, H.; Tao, X.; Li, W. Interfacial Structure Design of MXene-Based Nanomaterials for Electrochemical Energy Storage and Conversion. *InfoMat* **2020**, *2* (6), 1057–1076.
- (69) Yang, S.; Zhang, P.; Wang, F.; Ricciardulli, A. G.; Lohe, M. R.; Blom, P. W. M.; Feng, X. Fluoride-Free Synthesis of Two-Dimensional Titanium Carbide (MXene) Using a Binary Aqueous System. *Angew. Chem.* **2018**, *130* (47), 15717–15721.
- (70) Liu, L.; Yin, H.; Guo, W.; Jia, B.; Jiang, H. High Gravimetric Capacitance MXene Supercapacitor Electrode Based on Etched Ti₃C₂T_x by Chemical Etching. *Adv. Eng. Mater.* **2023**, *25*, 1–8.
- (71) Zhang, L.; Song, W.; Liu, H.; Ding, H.; Yan, Y.; Chen, R. Influencing Factors on Synthesis and Properties of MXene: A Review. *Processes* **2022**, *10* (9), 1744.
- (72) Cui, C.; Hu, M.; Zhang, C.; Cheng, R.; Yang, J.; Wang, X. High-Capacitance Ti₃C₂T_x MXene Obtained by Etching Submicron Ti₃AlC₂ Grains Grown in Molten Salt. *Chem. Commun.* **2018**, *54* (58), 8132–8135.
- (73) Kamysbayev, V.; Filatov, A. S.; Hu, H.; Rui, X.; Lagunas, F.; Wang, D.; Klie, R. F.; Talapin, D. V. Covalent Surface Modifications and Superconductivity of Two-Dimensional Metal Carbide MXenes. *Science (80-)*. **2020**, *369* (6506), 979–983.
- (74) Noor, U.; Mughal, M. F.; Ahmed, T.; Farid, M. F.; Ammar, M.; Kulsum, U.; Saleem, A.; Naeem, M.; Khan, A.; Sharif, A.; Waqar, K. Synthesis and applications of MXene-based composites: a review. *Nanotechnology* **2023**, *34*, 262001.
- (75) Wu, M.; Wang, B.; Hu, Q.; Wang, L.; Zhou, A. The Synthesis Process and Thermal Stability of V₂C MXene. *Materials (Basel)*. **2018**, *11*, 2112.
- (76) Zhou, C.; Zhao, X.; Xiong, Y.; Tang, Y.; Ma, X.; Tao, Q.; Sun, C.; Xu, W. A Review of Etching Methods of MXene and Applications of MXene Conductive Hydrogels. *Eur. Polym. J.* **2022**, *167*, 111063.
- (77) Chen, J.; Chen, M.; Zhou, W.; Xu, X.; Liu, B.; Zhang, W.; Wong, C. Simplified Synthesis of Fluoride-Free Ti₃C₂T_x via Electrochemical Etching toward High-Performance Electrochemical Capacitors. *ACS Nano* **2022**, *16* (2), 2461–2470.
- (78) Xu, C.; Wang, L.; Liu, Z.; Chen, L.; Guo, J.; Kang, N.; Ma, X. L.; Cheng, H. M.; Ren, W. Large-Area High-Quality 2D Ultrathin Mo₂C Superconducting Crystals. *Nat. Mater.* **2015**, *14* (11), 1135–1141.
- (79) Xiao, X.; Yu, H.; Jin, H.; Wu, M.; Fang, Y.; Sun, J.; Hu, Z.; Li, T.; Wu, J.; Huang, L.; Gogotsi, Y.; Zhou, J. Salt-Templated Synthesis of 2D Metallic MoN and Other Nitrides. *ACS Nano* **2017**, *11* (2), 2180–2186.
- (80) Zhang, F.; Zhang, Z.; Wang, H.; Chan, C. H.; Chan, N. Y.; Chen, X. X.; Dai, J. Y. Plasma-Enhanced Pulsed-Laser Deposition of Single-Crystalline Mo₂C Ultrathin Superconducting Films. *Phys. Rev. Mater.* **2017**, *1* (3), 1–8.
- (81) Xu, S.; Wei, G.; Li, J.; Ji, Y.; Klyui, N.; Izotov, V.; Han, W. Binder-Free Ti₃C₂T_x MXene Electrode Film for Supercapacitor Produced by Electrophoretic Deposition Method. *Chemical Engineering Journal* **2017**, *317*, 1026.
- (82) Yoon, Y.; Le, T. A.; Tiwari, A. P.; Kim, I.; Barsoum, M. W.; Lee, H. Low Temperature Solution Synthesis of Reduced Two Dimensional Ti₃C₂MXenes with Paramagnetic Behaviour. *Nanoscale* **2018**, *10* (47), 22429–22438.
- (83) Lin, H.; Gao, S.; Dai, C.; Chen, Y.; Shi, J. A Two-Dimensional Biodegradable Niobium Carbide (MXene) for Photothermal Tumor Eradication in NIR-I and NIR-II Biowindows. *J. Am. Chem. Soc.* **2017**, *139* (45), 16235–16247.
- (84) Meshkian, R.; Näslund, L. Å.; Halim, J.; Lu, J.; Barsoum, M. W.; Rosen, J. Synthesis of Two-Dimensional Molybdenum Carbide, Mo₂C, from the Gallium Based Atomic Laminate Mo₂Ga₂C. *Scr. Mater.* **2015**, *108*, 147–150.
- (85) Naguib, M.; Unocic, R. R.; Armstrong, B. L.; Nanda, J. Large-Scale Delamination of Multi-Layers Transition Metal Carbides and Carbonitrides “MXenes”. *Dalt. Trans.* **2015**, *44* (20), 9353–9358.
- (86) Halim, J.; Lukatskaya, M. R.; Cook, K. M.; Lu, J.; Smith, C. R.; Näslund, L. Å.; May, S. J.; Hultman, L.; Gogotsi, Y.; Eklund, P.; Barsoum, M. W. Transparent Conductive Two-Dimensional Titanium Carbide Epitaxial Thin Films. *Chem. Mater.* **2014**, *26* (7), 2374–2381.
- (87) Xie, X.; Xue, Y.; Li, L.; Chen, S.; Nie, Y.; Ding, W.; Wei, Z. Surface Al Leached Ti₃AlC₂ as a Substitute for Carbon for Use as a Catalyst Support in a Harsh Corrosive Electrochemical System. *Nanoscale* **2014**, *6* (19), 11035–11040.
- (88) Li, L.; Li, G.; Tan, L.; Zhang, Y.; Wu, B. Highly Efficiently Delaminated Single-Layered MXene Nanosheets with Large Lateral Size. *Langmuir* **2017**, *33* (36), 9000–9006.
- (89) Xuan, J.; Wang, Z.; Chen, Y.; Liang, D.; Cheng, L.; Yang, X.; Liu, Z.; Ma, R.; Sasaki, T.; Geng, F. Organic-Base-Driven Intercalation and Delamination for the Production of Functionalized Titanium Carbide Nanosheets with Superior Photothermal Therapeutic Performance. *Angew. Chem.* **2016**, *128* (47), 14789–14794.
- (90) Urbankowski, P.; Anasori, B.; Makaryan, T.; Er, D.; Kota, S.; Walsh, P. L.; Zhao, M.; Shenoy, V. B.; Barsoum, M. W.; Gogotsi, Y. Synthesis of Two-Dimensional Titanium Nitride Ti₄N₃ (MXene). *Nanoscale* **2016**, *8* (22), 11385–11391.
- (91) Sun, W.; Shah, S. A.; Chen, Y.; Tan, Z.; Gao, H.; Habib, T.; Radovic, M.; Green, M. J. Electrochemical Etching of Ti₂AlC to Ti₂CT_x (MXene) in Low-Concentration Hydrochloric Acid Solution. *J. Mater. Chem. A* **2017**, *5* (41), 21663–21668.
- (92) Cao, Y.; Guo, C.; Zou, Y. Rapid Synthesis of MXenes at Room Temperature. *Mater. Sci. Technol. (United Kingdom)* **2019**, *35* (15), 1904–1907.
- (93) Xu, X.; Zhang, Y.; Sun, H.; Zhou, J.; Yang, F.; Li, H.; Chen, H.; Chen, Y.; Liu, Z.; Qiu, Z.; Wang, D.; Ma, L.; Wang, J.; Zeng, Q.; Peng,

- Z. Progress and Perspective: MXene and MXene-Based Nanomaterials for High-Performance Energy Storage Devices. *Adv. Electron. Mater.* **2021**, *7* (7), 1–16.
- (94) Eklund, P.; Rosen, J.; Persson, P. O. A. Layered Ternary Mn +1AX_n Phases and Their 2D Derivative MXene: An Overview from a Thin-Film Perspective. *J. Phys. D: Appl. Phys.* **2017**, *50* (11), 113001.
- (95) Tran, M. H.; Schäfer, T.; Shahraei, A.; Dürrschnabel, M.; Molina-Luna, L.; Kramm, U. I.; Birkel, C. S. Adding a New Member to the MXene Family: Synthesis, Structure, and Electrocatalytic Activity for the Hydrogen Evolution Reaction of V₄C₃T_x. *ACS Appl. Energy Mater.* **2018**, *1* (8), 3908–3914.
- (96) Shimada, T.; Takenaka, N.; Ando, Y.; Otani, M.; Okubo, M.; Yamada, A. Relationship between Electric Double-Layer Structure of MXene Electrode and Its Surface Functional Groups. *Chem. Mater.* **2022**, *34* (5), 2069–2075.
- (97) Hu, T.; Wang, J.; Zhang, H.; Li, Z.; Hu, M.; Wang, X. Vibrational Properties of Ti₃C₂ and Ti₃C₂T₂ (T = O, F, OH) Monosheets by First-Principles Calculations: A Comparative Study. *Phys. Chem. Chem. Phys.* **2015**, *17* (15), 9997–10003.
- (98) Mahmood, M.; Rasheed, A.; Ayman, I.; Rasheed, T.; Munir, S.; Ajmal, S.; Agboola, P. O.; Warsi, M. F.; Shahid, M. Synthesis of Ultrathin MnO₂nanowire-Intercalated 2D-MXenes for High-Performance Hybrid Supercapacitors. *Energy Fuels* **2021**, *35* (4), 3469–3478.
- (99) Khazaei, M.; Arai, M.; Sasaki, T.; Chung, C. Y.; Venkataramanan, N. S.; Estili, M.; Sakka, Y.; Kawazoe, Y. Novel Electronic and Magnetic Properties of Two-Dimensional Transition Metal Carbides and Nitrides. *Adv. Funct. Mater.* **2013**, *23* (17), 2185–2192.
- (100) Abdah, M. A. A. M.; Awan, H. T. A.; Mehar, M.; Mustafa, M. N.; Walvekar, R.; Alam, M. W.; Khalid, M.; Umaphathi, R.; Chaudhary, V. Advancements in MXene-Polymer Composites for High-Performance Supercapacitor Applications. *J. Energy Storage* **2023**, *63* (March), 106942.
- (101) Naguib, M.; Mashtalir, O.; Carle, J.; Presser, V.; Lu, J.; Hultman, L.; Gogotsi, Y.; Barsoum, M. W. Two-Dimensional Transition Metal Carbides. *ACS Nano* **2012**, *6* (2), 1322–1331.
- (102) Ibrahim, Y.; Mohamed, A.; Abdelgawad, A. M.; Eid, K.; Abdullah, A. M.; Elzatahry, A. The Recent Advances in the Mechanical Properties of Self-Standing Two-Dimensional MXene-Based Nanostructures: Deep Insights into the Supercapacitor. *Nanomaterials* **2020**, *10*, 1916.
- (103) Sohan, A.; Banoth, P.; Aleksandrova, M.; Nirmala Grace, A.; Kollu, P. Review on MXene Synthesis, Properties, and Recent Research Exploring Electrode Architecture for Supercapacitor Applications. *Int. J. Energy Res.* **2021**, *45* (14), 19746–19771.
- (104) Ying, G.; Kota, S.; Dillon, A. D.; Fafarman, A. T.; Barsoum, M. W. Conductive transparent V₂C₂x (MXene) films. *FlatChem* **2018**, *8* (March), 25.
- (105) Hu, T.; Yang, J.; Li, W.; Wang, X.; Li, C. M. Quantifying the rigidity of 2D carbides (MXenes). *Phys. Chem. Chem. Phys.* **2020**, *22*, 2115.
- (106) Cheng, R.; Hu, T.; Hu, M.; Li, C.; Liang, Y.; Wang, Z.; Zhang, H.; Li, M.; Wang, H.; Lu, H.; Fu, Y.; Zhang, H.; Yang, Q. H.; Wang, X. MXenes Induce Epitaxial Growth of Size-Controlled Noble Nanometals: A Case Study for Surface Enhanced Raman Scattering (SERS). *J. Mater. Sci. Technol.* **2020**, *40*, 119–127.
- (107) Mathis, T. S.; Maleski, K.; Goad, A.; Sarycheva, A.; Anayee, M.; Foucher, A. C.; Hantanasirisakul, K.; Shuck, C. E.; Stach, E. A.; Gogotsi, Y. Modified MAX Phase Synthesis for Environmentally Stable and Highly Conductive Ti₃C₂MXene. *ACS Nano* **2021**, *15* (4), 6420–6429.
- (108) Zhang, J.; Kong, N.; Hegh, D.; Usman, K. A. S.; Guan, G.; Qin, S.; Jurewicz, I.; Yang, W.; Razal, J. M. Freezing Titanium Carbide Aqueous Dispersions for Ultra-Long-Term Storage. *ACS Appl. Mater. Interfaces* **2020**, *12* (30), 34032–34040.
- (109) Huang, W.; Hu, L.; Tang, Y.; Xie, Z.; Zhang, H. Recent Advances in Functional 2D MXene-Based Nanostructures for Next-Generation Devices. *Adv. Funct. Mater.* **2020**, *30* (49), 1–32.
- (110) Ferrara, C.; Gentile, A.; Marchionna, S.; Ruffo, R. Ti₃C₂T_x MXene Compounds for Electrochemical Energy Storage. *Curr. Opin. Electrochem.* **2021**, *29*, 100764.
- (111) Xu, J.; Peng, T.; Zhang, Q.; Zheng, H.; Yu, H.; Shi, S. Intercalation Effects on the Electrochemical Properties of Ti₃C₂T_xMXene Nanosheets for High-Performance Supercapacitors. *ACS Appl. Nano Mater.* **2022**, *5* (7), 8794–8803.
- (112) Shahzad, F.; Zaidi, S. A.; Naqvi, R. A. 2D Transition Metal Carbides (MXene) for Electrochemical Sensing: A Review. *Crit. Rev. Anal. Chem.* **2022**, *52* (4), 848–864.
- (113) Chen, C.; Boota, M.; Urbankowski, P.; Anasori, B.; Miao, L.; Jiang, J.; Gogotsi, Y. Effect of Glycine Functionalization of 2D Titanium Carbide (MXene) on Charge Storage. *J. Mater. Chem. A* **2018**, *6* (11), 4617–4622.
- (114) Bao, Z.; Lu, C.; Cao, X.; Zhang, P.; Yang, L.; Zhang, H.; Sha, D.; He, W.; Zhang, W.; Pan, L.; Sun, Z. Role of MXene Surface Terminations in Electrochemical Energy Storage: A Review. *Chin. Chem. Lett.* **2021**, *32* (9), 2648–2658.
- (115) Nasrin, K.; Sudharshan, V.; Arunkumar, M.; Sathish, M. 2D/2D Nanoarchitected Nb₂C/Ti₃C₂MXene Heterointerface for High-Energy Supercapacitors with Sustainable Life Cycle. *ACS Appl. Mater. Interfaces* **2022**, *14*, 21038.
- (116) Jiang, T.; Wang, Y.; Chen, G. Z. Electrochemistry of Titanium Carbide MXenes in Supercapacitor. *Small Methods* **2023**, *7*, 1–21.
- (117) Liu, S.; Kang, L.; Zhang, J.; Jun, S. C.; Yamauchi, Y. Carbonaceous Anode Materials for Non-Aqueous Sodium- And Potassium-Ion Hybrid Capacitors. *ACS Energy Lett.* **2021**, *6* (11), 4127–4154.
- (118) Liu, S.; Kang, L.; Hu, J.; Jung, E.; Henzie, J.; Alowasheer, A.; Zhang, J.; Miao, L.; Yamauchi, Y.; Jun, S. C. Realizing Superior Redox Kinetics of Hollow Bimetallic Sulfide Nanoarchitectures by Defect-Induced Manipulation toward Flexible Solid-State Supercapacitors. *Small* **2022**, DOI: 10.1002/smll.202104507.
- (119) Zhang, X.; Zhang, H.; Li, C.; Wang, K.; Sun, X.; Ma, Y. Recent Advances in Porous Graphene Materials for Supercapacitor Applications. *RSC Adv.* **2014**, *4* (86), 45862–45884.
- (120) Kandasamy, M.; Sahoo, S.; Nayak, S. K.; Chakraborty, B.; Rout, C. S. Recent advances in engineered metal oxide nanostructures for supercapacitor applications: experimental and theoretical aspects. *J. Mater. Chem. A* **2021**, *9*, 17643–17700.
- (121) Zhang, Y.; El-demellawi, J. K.; Jiang, Q.; Ge, G.; Liang, H.; Lee, K.; Dong, X.; Alshareef, H. N. MXene hydrogels: fundamentals and applications. *Chem. Soc. Rev.* **2020**, *49*, 7229.
- (122) Jiang, Q.; Lei, Y.; Liang, H.; Xi, K.; Xia, C.; Alshareef, H. N. Review of MXene Electrochemical Microsupercapacitors. *Energy Storage Mater.* **2020**, *27*, 78–95.
- (123) Wang, X.; Mathis, T. S.; Li, K.; Lin, Z.; Vlcek, L.; Torita, T.; Osti, N. C.; Hatter, C.; Urbankowski, P.; Sarycheva, A.; Tyagi, M.; Mamontov, E.; Simon, P.; Gogotsi, Y. Influences from Solvents on Charge Storage in Titanium Carbide MXenes. *Nat. Energy* **2019**, *4* (3), 241–248.
- (124) Liang, C.; Meng, Y.; Zhang, Y.; Zhang, H.; Wang, W.; Lu, M.; Wang, G. Insights into the Impact of Interlayer Spacing on MXene-Based Electrodes for Supercapacitors: A Review. *J. Energy Storage* **2023**, *65*, 107341.
- (125) Li, C.; Wang, S.; Cui, Y.; Wang, X.; Yong, Z.; Liang, D.; Chi, Y.; Wang, Z. Sandwich-like MXene/ α -Fe₂O₃-C-MoS₂-PEDOT:PSS/MXene Film Electrodes with Ultrahigh Area Capacitance for Flexible Supercapacitors. *ACS Appl. Mater. Interfaces* **2022**, *14* (7), 9172–9182.
- (126) Li, K.; Zhang, P.; Soomro, R. A.; Xu, B. Alkali-Induced Porous MXene/Carbon Nanotube-Based Film Electrodes for Supercapacitors. *ACS Appl. Nano Mater.* **2022**, *5* (3), 4180–4186.
- (127) Gandla, D.; Zhang, F.; Tan, D. Q. Advantage of Larger Interlayer Spacing of a Mo₂Ti₃C₃MXene Free-Standing Film Electrode toward an Excellent Performance Supercapacitor in a Binary Ionic Liquid-Organic Electrolyte. *ACS Omega* **2022**, *7* (8), 7190–7198.
- (128) Liu, Y.; Zhou, H.; Zhou, W.; Meng, S.; Qi, C.; Liu, Z.; Kong, T. Biocompatible, High-Performance, Wet-Adhesive, Stretchable All-Hydrogel Supercapacitor Implant Based on PANI@rGO/Mxenes

- Electrode and Hydrogel Electrolyte. *Adv. Energy Mater.* **2021**, *11* (30), 1–11.
- (129) Nahirniak, S.; Ray, A.; Saruhan, B. Challenges and Future Prospects of the MXene-Based Materials for Energy Storage Applications. *Batteries* **2023**, *9* (2), 126.
- (130) Han, M.; Shuck, C. E.; Rakhmanov, R.; Parchment, D.; Anasori, B.; Koo, C. M.; Friedman, G.; Gogotsi, Y. Beyond Ti₃C₂T_x: MXenes for Electromagnetic Interference Shielding. *ACS Nano* **2020**, *14* (4), 5008–5016.
- (131) Luo, Y.; Yang, C.; Tian, Y.; Tang, Y.; Yin, X.; Que, W. A Long Cycle Life Asymmetric Supercapacitor Based on Advanced Nickel-Sulfide/Titanium Carbide (MXene) Nanohybrid and MXene Electrodes. *Journal of Power Sources*. **2020**, *450*, 227694.
- (132) Li, J.; Xu, S.; Li, Y.; Wan, L.; Wei, G.; Jiang, T.; Li, Z.; Yang, Y. Suppressing the Self-Discharge of MXene-Based Supercapacitors by Liquid Crystal Additive. *Nano Energy* **2023**, *115*, 108754.
- (133) Yeom, C.; Chen, K.; Kiriya, D.; Yu, Z.; Cho, G.; Javey, A. Large-Area Compliant Tactile Sensors Using Printed Carbon Nanotube Active-Matrix Backplanes. *Adv. Mater.* **2015**, *27* (9), 1561–1566.
- (134) Li, H.; Hou, Y.; Wang, F.; Lohe, M. R.; Zhuang, X.; Niu, L.; Feng, X. Flexible All-Solid-State Supercapacitors with High Volumetric Capacitances Boosted by Solution Processable MXene and Electrochemically Exfoliated Graphene. *Adv. Energy Mater.* **2017**, *7* (4), 2–7.
- (135) Kumar, S.; Rehman, M. A.; Lee, S.; Kim, M.; Hong, H.; Park, J. Y.; Seo, Y. Supercapacitors Based on Ti₃C₂T_x MXene Extracted from Supernatant and Current Collectors Passivated by CVD-Graphene. *Sci. Rep.* **2021**, *11* (1), 1–9.
- (136) Sikdar, A.; Dutta, P.; Deb, S. K.; Majumdar, A.; Padma, N.; Ghosh, S.; Maiti, U. N. Spontaneous Three-Dimensional Self-Assembly of MXene and Graphene for Impressive Energy and Rate Performance Pseudocapacitors. *Electrochim. Acta* **2021**, *391*, 138959.
- (137) Zheng, X.; Nie, W.; Hu, Q.; Wang, X.; Wang, Z.; Zou, L.; Hong, X.; Yang, H.; Shen, J.; Li, C. Multifunctional RGO/Ti₃C₂T_x MXene Fabrics for Electrochemical Energy Storage, Electromagnetic Interference Shielding, Electrothermal and Human Motion Detection. *Mater. Des.* **2021**, *200*, 109442.
- (138) Zhang, M.; Cao, J.; Wang, Y.; Song, J.; Jiang, T.; Zhang, Y.; Si, W.; Li, X.; Meng, B.; Wen, G. Electrolyte-Mediated Dense Integration of Graphene-MXene Films for High Volumetric Capacitance Flexible Supercapacitors. *Nano Res.* **2021**, *14* (3), 699–706.
- (139) Ren, C. E.; Zhao, M. Q.; Makaryan, T.; Halim, J.; Boota, M.; Kota, S.; Anasori, B.; Barsoum, M. W.; Gogotsi, Y. Porous Two-Dimensional Transition Metal Carbide (MXene) Flakes for High-Performance Li-Ion Storage. *ChemElectroChem*. **2016**, *3* (5), 689–693.
- (140) Park, J. W.; Lee, D. Y.; Kim, H.; Hyeon, J. S.; de Andrade, M. J.; Baughman, R. H.; Jeong Kim, S. Highly Loaded MXene/Carbon Nanotube Yarn Electrodes for Improved Asymmetric Supercapacitor Performance. *MRS Commun.* **2019**, *9* (1), 114–121.
- (141) Wang, R.; Luo, S.; Xiao, C.; Chen, Z.; Li, H.; Asif, M.; Chan, V.; Liao, K.; Sun, Y. MXene-Carbon Nanotubes Layer-by-Layer Assembly Based on-Chip Micro-Supercapacitor with Improved Capacitive Performance. *Electrochim. Acta* **2021**, *386*, 138420.
- (142) Li, S.; Zhang, Q.; Liu, L.; Wang, J.; Zhang, L.; Shi, M.; Chen, X. Ultra-Stable Sandwich Shaped Flexible MXene/CNT@Ni Films for High Performance Supercapacitor. *J. Alloys Compd.* **2023**, *941*, 168963.
- (143) Wu, Z.; Zhu, Y.; Ji, X.; Banks, C. E. *Transition Metal Oxides as Supercapacitor Materials*. **2016**, 317–344.
- (144) Zhao, M. Q.; Torelli, M.; Ren, C. E.; Ghidui, M.; Ling, Z.; Anasori, B.; Barsoum, M. W.; Gogotsi, Y. 2D Titanium Carbide and Transition Metal Oxides Hybrid Electrodes for Li-Ion Storage. *Nano Energy* **2016**, *30*, 603–613.
- (145) Wang, J.; Gong, J.; Zhang, H.; Lv, L.; Liu, Y.; Dai, Y. Construction of Hexagonal Nickel-Cobalt Oxide Nanosheets on Metal-Organic Frameworks Based on MXene Interlayer Ion Effect for Hybrid Supercapacitors. *J. Alloys Compd.* **2021**, *870*, 159466.
- (146) Zhu, J.; Tang, Y.; Yang, C.; Wang, F.; Cao, M. Composites of TiO₂ Nanoparticles Deposited on Ti₃C₂ MXene Nanosheets with Enhanced Electrochemical Performance. *J. Electrochem. Soc.* **2016**, *163* (5), A785–A791.
- (147) Luo, W.; Sun, Y.; Han, Y.; Ding, J.; Li, T.; Hou, C.; Ma, Y. Flexible Ti₃C₂T_x MXene/Polypyrrole Composite Films for High-Performance All-Solid Asymmetric Supercapacitors. *Electrochim. Acta* **2023**, *441*, 141818.
- (148) Rakhi, R. B.; Ahmed, B.; Anjum, D.; Alshareef, H. N. Direct Chemical Synthesis of MnO₂ Nanowhiskers on Transition-Metal Carbide Surfaces for Supercapacitor Applications. *ACS Appl. Mater. Interfaces* **2016**, *8* (29), 18806–18814.
- (149) Zou, R.; Quan, H.; Pan, M.; Zhou, S.; Chen, D.; Luo, X. Self-Assembled MXene(Ti₃C₂T_x)/α-Fe₂O₃ Nanocomposite as Negative Electrode Material for Supercapacitors. *Electrochim. Acta* **2018**, *292*, 31–38.
- (150) Ammar, A. U.; Bakan-Misirlioglu, F.; Aleinawi, M. H.; Franzo, G.; Condorelli, G. G.; Yesilbag, F. N. T.; Yesilbag, Y. O.; Mirabella, S.; Erdem, E. All-in-One Supercapacitors with High Performance Enabled by Mn/Cu Doped ZnO and MXene. *Mater. Res. Bull.* **2023**, *165* (March), 112334.
- (151) Zhang, Y.; Cao, J.; Yuan, Z.; Zhao, L.; Wang, L.; Han, W. Assembling Co₃O₄ Nanoparticles into MXene with Enhanced Electrochemical Performance for Advanced Asymmetric Supercapacitors. *J. Colloid Interface Sci.* **2021**, *599*, 109–118.
- (152) Zhang, K.; Ying, G.; Liu, L.; Ma, F.; Su, L.; Zhang, C.; Wu, D.; Wang, X.; Zhou, Y. Three-Dimensional Porous Ti₃C₂T_x-NiO Composite Electrodes with Enhanced Electrochemical Performance for Supercapacitors. *Materials (Basel)*. **2019**, *12* (1), 188.
- (153) Zhang, X.; Shao, B.; Guo, A.; Gao, Z.; Qin, Y.; Zhang, C.; Cui, F.; Yang, X. Improved Electrochemical Performance of CoOx-NiO/Ti₃C₂T_x MXene Nanocomposites by Atomic Layer Deposition towards High Capacitance Supercapacitors. *J. Alloys Compd.* **2021**, *862*, 158546.
- (154) Bin, X.; Tian, Y.; Luo, Y.; Sheng, M.; Luo, Y.; Ju, M.; Que, W. High-Performance Flexible and Free-Standing N-Doped Ti₃C₂T_x/MoO_x Films as Electrodes for Supercapacitors. *Electrochim. Acta* **2021**, *389*, 138774.
- (155) Ma, W.; Sui, Y.; Ye, Y.; Ma, Y.; Zhang, P.; Duan, N.; Song, Z.; Qin, C. Self-Standing Ti₃C₂T_x/MoO₃-XComposite Films with High Volumetric and Gravimetric Capacitance Performances for Flexible Solid-State Supercapacitors. *Energy Fuels* **2022**, *36* (12), 6532–6541.
- (156) Pan, Z.; Yang, C.; Chen, Z.; Ji, X. Construction of Ti₃C₂T_x/WO_x Heterostructures on Carbon Cloth for Ultrahigh-Mass Loading Flexible Supercapacitor. *Nano Res.* **2022**, *15*, 8991–8999.
- (157) Darmiani, N.; Irajizad, A.; Esfandiari, A.; Asen, P. Cauliflower-Like Ni/MXene-Bridged Fiber-Shaped Electrode for Flexible Micro-supercapacitor. *Energy Fuels* **2022**, *36* (4), 2140–2148.
- (158) Gao, L.; Li, C.; Huang, W.; Mei, S.; Lin, H.; Ou, Q.; Zhang, Y.; Guo, J.; Zhang, F.; Xu, S.; Zhang, H. MXene/Polymer Membranes: Synthesis, Properties, and Emerging Applications. *Chem. Mater.* **2020**, *32* (5), 1703–1747.
- (159) Chen, J.; Liu, B.; Cai, H.; Liu, S.; Yamauchi, Y.; Jun, S. C. Covalently Interlayer-Confined Organic-Inorganic Heterostructures for Aqueous Potassium Ion Supercapacitors. *Small*. **2023**, DOI: 10.1002/smll.202204275.
- (160) Yang, Q.; Wang, Y.; Li, X.; Li, H.; Wang, Z.; Tang, Z.; Ma, L.; Mo, F.; Zhi, C. *Recent Progress of MXene-Based Nanomaterials in Flexible Energy Storage and Electronic Devices*. **2018**, *1*, 183–195.
- (161) Ling, Z.; Ren, C. E.; Zhao, M. Q.; Yang, J.; Giammarco, J. M.; Qiu, J.; Barsoum, M. W.; Gogotsi, Y. Flexible and Conductive MXene Films and Nanocomposites with High Capacitance. *Proc. Natl. Acad. Sci. U. S. A.* **2014**, *111* (47), 16676–16681.
- (162) Yan, J.; Ma, Y.; Zhang, C.; Li, X.; Liu, W.; Yao, X.; Yao, S.; Luo, S. Polypyrrole-MXene Coated Textile-Based Flexible Energy Storage Device. *RSC Adv.* **2018**, *8* (69), 39742–39748.
- (163) Naguib, M.; Saito, T.; Lai, S.; Rager, M. S.; Aytug, T.; Parans Paranthaman, M.; Zhao, M.-Q.; Gogotsi, Y. Ti₃C₂T_x (MXene)-polyacrylamide nanocomposite films. *RSC Adv.* **2016**, *6*, 72069.
- (164) Zhu, M.; Huang, Y.; Deng, Q.; Zhou, J.; Pei, Z.; Xue, Q.; Huang, Y.; Wang, Z.; Li, H.; Huang, Q.; Zhi, C. Highly Flexible, Freestanding Supercapacitor Electrode with Enhanced Performance Obtained by

- Hybridizing Polypyrrole Chains with MXene. *Adv. Energy Mater.* **2016**, DOI: 10.1002/aenm.201600969.
- (165) Zhang, M.; Héraly, F.; Yi, M.; Yuan, J. Multitasking Tartaric-Acid-Enabled, Highly Conductive, and Stable MXene/Conducting Polymer Composite for Ultrafast Supercapacitor. *Cell Reports Phys. Sci.* **2021**, *2* (6), 100449.
- (166) Vahidmohammadi, A.; Moncada, J.; Chen, H.; Kayali, E.; Orangi, J.; Carrero, C. A.; Beidaghi, M. Thick and Freestanding MXene/PANI Pseudocapacitive Electrodes with Ultrahigh Specific Capacitance. *J. Mater. Chem. A* **2018**, *6* (44), 22123–22133.
- (167) Zheng, X.; Wang, Y.; Nie, W.; Wang, Z.; Hu, Q.; Li, C.; Wang, P.; Wang, W. Elastic Polyaniline Nanoarrays/MXene Textiles for All-Solid-State Supercapacitors and Anisotropic Strain Sensors. *Compos. Part A Appl. Sci. Manuf.* **2022**, *158*, 106985.
- (168) Ye, F.; Xu, B.; Chen, R.; Li, R.; Chang, G. A High Performance Flexible Cotton-Based Supercapacitor Prepared by in-Situ Polyaniline and MXene Coating. *J. Energy Storage* **2023**, *62*, 106803.
- (169) Chang, L.; Peng, Z.; Zhang, T.; Yu, C.; Zhong, W. *Mechanical Strength Constructed from MXenes*. **2021**, *13*, 3079–3091.
- (170) Zhao, M. Q.; Ren, C. E.; Ling, Z.; Lukatskaya, M. R.; Zhang, C.; Van Aken, K. L.; Barsoum, M. W.; Gogotsi, Y. Flexible MXene/Carbon Nanotube Composite Paper with High Volumetric Capacitance. *Adv. Mater.* **2015**, *27* (2), 339–345.
- (171) Wang, Y.; Chen, N.; Liu, Y.; Zhou, X.; Pu, B.; Qing, Y.; Zhang, M.; Jiang, X.; Huang, J.; Tang, Q.; Zhou, B.; Yang, W. MXene/Graphdiyne Nanotube Composite Films for Free-Standing and Flexible Solid-State Supercapacitor. *Chem. Eng. J.* **2022**, *450* (P4), 138398.
- (172) Dall'Agnese, Y.; Lukatskaya, M. R.; Cook, K. M.; Taberna, P. L.; Gogotsi, Y.; Simon, P. High Capacitance of Surface-Modified 2D Titanium Carbide in Acidic Electrolyte. *Electrochem. Commun.* **2014**, *48*, 118–122.
- (173) Wang, X.; Garnero, C.; Rochard, G.; Magne, D.; Morisset, S.; Hurand, S.; Chartier, P.; Rousseau, J.; Cabioch, T.; Coutanceau, C.; Mauchamp, V.; Célérier, S. A New Etching Environment (FeF₃/HCl) for the Synthesis of Two-Dimensional Titanium Carbide MXenes: A Route towards Selective Reactivity: Vs. Water. *J. Mater. Chem. A* **2017**, *5* (41), 22012–22023.
- (174) Najam, T.; Shah, S. S. A.; Peng, L.; Javed, M. S.; Imran, M.; Zhao, M.-Q.; Tsiakaras, P. Synthesis and Nano-Engineering of MXenes for Energy Conversion and Storage Applications: Recent Advances and Perspectives. *Coord. Chem. Rev.* **2022**, *454*, 214339.
- (175) Shen, L.; Zhou, X.; Zhang, X.; Zhang, Y.; Liu, Y.; Wang, W.; Si, W.; Dong, X. Carbon-Intercalated Ti₃C₂T_x MXene for High-Performance Electrochemical Energy Storage. *J. Mater. Chem. A* **2018**, *6* (46), 23513–23520.
- (176) Ronchi, R. M.; Arantes, J. T.; Santos, S. F. Synthesis, Structure, Properties and Applications of MXenes: Current Status and Perspectives. *Ceram. Int.* **2019**, *45* (15), 18167–18188.
- (177) Tang, J.; Mathis, T.; Zhong, X.; Xiao, X.; Wang, H.; Anayee, M.; Pan, F.; Xu, B.; Gogotsi, Y. Optimizing Ion Pathway in Titanium Carbide MXene for Practical High-Rate Supercapacitor. *Adv. Energy Mater.* **2021**, *11* (4), 1–8.
- (178) Tang, J.; Yi, W.; Zhong, X.; Zhang, C.; Xiao, X.; Pan, F.; Xu, B. Laser Writing of the Restacked Titanium Carbide MXene for High Performance Supercapacitors. *Energy Storage Mater.* **2020**, *32* (May), 418–424.
- (179) Wang, X.; Lin, S.; Tong, H.; Huang, Y.; Tong, P.; Zhao, B.; Dai, J.; Liang, C.; Wang, H.; Zhu, X.; Sun, Y.; Dou, S. Electrochimica Acta Two-Dimensional V₄C₃ MXene as High Performance Electrode Materials for Supercapacitors. *Electrochim. Acta* **2019**, *307*, 414–421.
- (180) Persson, I.; el Ghazaly, A.; Tao, Q.; Halim, J.; Kota, S.; Darakchieva, V.; Palisaitis, J.; Barsoum, M. W.; Rosen, J.; Persson, P. O. Å. Tailoring Structure, Composition, and Energy Storage Properties of MXenes from Selective Etching of In-Plane, Chemically Ordered MAX Phases. *Small* **2018**, *14* (17), 1–7.
- (181) Murali, G.; Rawal, J.; Modigunta, J. K. R.; Park, Y. H.; Lee, J. H.; Lee, S. Y.; Park, S. J.; In, I. A Review on MXenes: New-Generation 2D Materials for Supercapacitors. *Sustain. Energy Fuels* **2021**, *5* (22), 5672–5693.
- (182) Hu, M.; Li, Z.; Hu, T.; Zhu, S.; Zhang, C.; Wang, X. High-Capacitance Mechanism for Ti₃C₂T_x MXene by in Situ Electrochemical Raman Spectroscopy Investigation. *ACS Nano* **2016**, *10* (12), 11344–11350.
- (183) Murugesan, R. A.; Nagamuthu Raja, K. C. Capacitance Performance of Ti₃C₂T_x MXene Nanosheets on Alkaline and Neutral Electrolytes. *Mater. Res. Bull.* **2023**, *163* (March), 112217.
- (184) Wang, X.; Wang, S.; Li, C.; Cui, Y.; Yong, Z.; Liang, D.; Chi, Y.; Wang, Z. ScienceDirect Flexible Supercapacitor Based on MXene Cross-Linked Organic Gel Electrolyte with Wide Working Temperature. *Int. J. Hydrogen Energy* **2023**, *48* (12), 4921–4930.
- (185) Lukatskaya, M. R.; Kota, S.; Lin, Z.; Zhao, M. Q.; Shpigel, N.; Levi, M. D.; Halim, J.; Taberna, P. L.; Barsoum, M. W.; Simon, P.; Gogotsi, Y. Ultra-High-Rate Pseudocapacitive Energy Storage in Two-Dimensional Transition Metal Carbides. *Nat. Energy* **2017**, *2* (8), 1–6.
- (186) Jiang, Q.; Kurra, N.; Alhabeab, M.; Gogotsi, Y.; Alshareef, H. N. All Pseudocapacitive MXene-RuO₂ Asymmetric Supercapacitors. *Adv. Energy Mater.* **2018**, *8* (13), 1–10.
- (187) Gogotsi, Y.; Penner, R. M. Energy Storage in Nanomaterials – Capacitive, Pseudocapacitive, or Battery-like? *ACS Nano* **2018**, *12*, 2081–2083.
- (188) Yan, F.; Zhang, C.; Wang, H.; Zhang, X.; Zhang, H.; Jia, H.; Zhao, Y.; Wang, J. A Coupled Conductor of Ionic Liquid with Ti₃C₂MXene to Improve Electrochemical Properties. *J. Mater. Chem. A* **2021**, *9* (1), 442–452.
- (189) Jäckel, N.; Krüner, B.; Van Aken, K. L.; Alhabeab, M.; Anasori, B.; Kaasik, F.; Gogotsi, Y.; Presser, V. Electrochemical in Situ Tracking of Volumetric Changes in Two-Dimensional Metal Carbides (MXenes) in Ionic Liquids. *ACS Appl. Mater. Interfaces* **2016**, *8* (47), 32089–32093.
- (190) Weng, Y.; Pan, H.; Wu, N.; Chen, G. Z. *AC SC. J. Power Sources* **2015**, *274*, 1118.
- (191) Wang, H.; Li, L.; Zhu, C.; Lin, S.; Wen, J.; Jin, Q.; Zhang, X. In Situ Polymerized Ti₃C₂T_x/PDA Electrode with Superior Areal Capacitance for Supercapacitors. *J. Alloys Compd.* **2019**, *778*, 858–865.
- (192) Huang, X.; Huang, J.; Yang, D.; Wu, P. A Multi-Scale Structural Engineering Strategy for High-Performance MXene Hydrogel Supercapacitor Electrode. *Adv. Sci.* **2021**, *8*, 1–9.
- (193) Su, X.; Zhang, J.; Mu, H.; Zhao, J.; Wang, Z.; Zhao, Z.; Han, C.; Ye, Z. Effects of Etching Temperature and Ball Milling on the Preparation and Capacitance of Ti₃C₂MXene. *J. Alloys Compd.* **2018**, *752*, 32–39.
- (194) Tang, J.; Mathis, T. S.; Kurra, N.; Sarycheva, A.; Xiao, X.; Hedhili, M. N.; Jiang, Q.; Alshareef, H. N.; Xu, B.; Pan, F.; Gogotsi, Y. Tuning the Electrochemical Performance of Titanium Carbide MXene by Controllable In Situ Anodic Oxidation. *Angew. Chem.* **2019**, *131* (49), 18013–18019.
- (195) Maleski, K.; Ren, C. E.; Zhao, M. Q.; Anasori, B.; Gogotsi, Y. Size-Dependent Physical and Electrochemical Properties of Two-Dimensional MXene Flakes. *ACS Appl. Mater. Interfaces* **2018**, *10* (29), 24491–24498.
- (196) Kayali, E.; VahidMohammadi, A.; Orangi, J.; Beidaghi, M. Controlling the Dimensions of 2D MXenes for Ultra-High-Rate Pseudocapacitive Energy Storage. *ACS Appl. Mater. Interfaces* **2018**, *10*, 25949.
- (197) Peng, Y. Y.; Akuzum, B.; Kurra, N.; Zhao, M. Q.; Alhabeab, M.; Anasori, B.; Kumbur, E. C.; Alshareef, H. N.; Ger, M. D.; Gogotsi, Y. All-MXene (2D Titanium Carbide) Solid-State Microsupercapacitors for on-Chip Energy Storage. *Energy Environ. Sci.* **2016**, *9* (9), 2847–2854.
- (198) Osti, N. C.; Naguib, M.; Ostadhosseine, A.; Xie, Y.; Kent, P. R. C.; Dyatkin, B.; Rother, G.; Heller, W. T.; Van Duin, A. C. T.; Gogotsi, Y.; Mamontov, E. Effect of Metal Ion Intercalation on the Structure of MXene and Water Dynamics on Its Internal Surfaces. *ACS Appl. Mater. Interfaces* **2016**, *8* (14), 8859–8863.
- (199) Okubo, M.; Sugahara, A.; Kajiyama, S.; Yamada, A. MXene as a Charge Storage Host. *Acc. Chem. Res.* **2018**, *51* (3), 591–599.